

Adaptive Relaxation based Non-Conservative Chance Constrained Stochastic MPC for Battery Scheduling Under Forecast Uncertainties

Avik Ghosh, Cristian Cortes-Aguirre, Yi-An Chen, Adil Khurram, and Jan Kleissl

Abstract—Chance constrained stochastic model predictive controllers (CC-SMPC) trade off full constraint satisfaction for economical plant performance under uncertainty. Previous CC-SMPC works are over-conservative in constraint violations leading to worse economic performance. Other past works require a-priori information about the uncertainty set, limiting their application to real-world systems. This paper considers a discrete linear time invariant system with hard constraints on inputs and chance constraints on states, with unknown uncertainty distribution, statistics, or samples. This work proposes a novel adaptive online update rule to relax the state constraints based on the time-average of past constraint violations, for the SMPC to achieve reduced conservativeness in closed-loop. Under an ideal control policy assumption, it is proven that the time-average of constraint violations converges to the maximum allowed violation probability. The time-average of constraint violations is also proven to asymptotically converge even without the simplifying assumptions. The proposed method is applied to the optimal battery energy storage system (BESS) dispatch in a grid connected microgrid with PV generation and load demand with chance constraints on BESS state-of-charge (SOC). Realistic simulations show the superior electricity cost saving potential of the proposed method as compared to the traditional MPC (with hard constraints on BESS SOC), by satisfying the chance constraints non-conservatively in closed-loop, thereby effectively trading off increased cost savings with minimal adverse effects on BESS lifetime.

Index Terms—Stochastic model predictive control, chance constraints, forecast uncertainty, discrete LTI systems, uncertainties, non-conservative, microgrids, battery energy storage systems

NOMENCLATURE

α	Maximum probability of violation of state constraints
γ	Constant of proportionality in online h update rule
\hat{w}	Width of the critical region
κ	Critical region
\mathbb{P}	Probability measure
\mathcal{F}_t	Filtration
\tilde{h}	Adaptive state constraint tightening parameter
A	System state transition matrix
B	System control input matrix
d	Control input coupling vector dimension
E	System state uncertainty matrix
F	Control input uncertainty matrix

G	State chance constraint matrix
g	State chance constraint vector
h	Adaptive state constraint relaxing parameter
k, t	Time index
M	Control input coupling matrix
m	Control input coupling vector / Control input dimension
N	MPC prediction horizon length
n	State dimension
p	Uncertainty dimension / Probability of violation of state constraints
q	Control input constraint vector dimension
r	State chance constraint vector dimension
S	Control input constraint matrix
s	Control input constraint vector
u	Control input
V	State constraint violation tracker
w	Uncertainty
x	State
Y	Time-average of state constraint violations
Z	Absolute difference between α and Y
BESS	Battery energy storage system
JCC	Joint chance constraints
LTI	Linear time invariant
MG	Microgrid
MPC	Model predictive control
NCDC	Non-coincident demand charge
OPDC	On-peak demand charge
PV	Photovoltaic
SMPC	Stochastic MPC
SOC	State-of-charge
VRES	Variable renewable energy sources

I. INTRODUCTION

A. Motivation

Currently, there is great emphasis on integrating variable renewable energy sources (VRES), such as wind and PV generators into the electricity grid, with the goal of de-carbonizing power production. There is, however, an intermittent nature to VRES, which can potentially lead to power imbalance in the electric grid, thereby risking grid stability [1]. Battery energy storage systems (BESS) can minimize power fluctuations caused by the integration of VRES into the grid [1], and can additionally be used for energy arbitrage, peak load shaving, valley-filling, and ancillary services. However, to maximize benefits from installing BESS, optimal BESS scheduling

A. Ghosh (*corresponding author*), C. Cortes-Aguirre, Y. Chen and A. Khurram are with the Department of Mechanical and Aerospace Engineering, University of California, San Diego, CA, 92093 USA (UCSD) email: {avghosh, ccortes, yic002, akhurram}@ucsd.edu. J. Kleissl is the Director of the Center for Energy Research in the Department of Mechanical and Aerospace Engineering at UCSD. email: jkleissl@ucsd.edu.

strategies need to be devised to maximize electricity bill savings, while providing services to the grid.

It is possible to optimally dispatch BESS, utilizing Model predictive control (MPC) based scheduling algorithms that include grid constraints. In MPC, an objective function (for example, electricity cost) is minimized to compute a sequence of optimal control inputs (i.e., BESS dispatch) based on forecasts of load and VRES, internal plant model (i.e., microgrid operational constraints), and initial system state (BESS state of charge) over a finite receding prediction horizon. The prediction horizon is divided into a specific number of time-steps. During execution, only the first computed control input of the prediction horizon is implemented, after which the system state evolves as it moves to the next time-step. Thereafter, forecasts are updated, and the MPC optimization is solved again from the new initial system state and time-step. However, uncertainty in forecasts can significantly reduce performance and should be taken into account when formulating MPCs.

Classical open-loop min-max formulation based robust MPC can be used to factor in uncertainty but it leads to over-conservative solutions which may not be economical from an operational perspective [2]. Other variations of robust MPC such as closed-loop min-max formulation (commonly known as “Feedback MPC”) suffer from prohibitive complexity [2]. Tube-based MPC requires specification of a bounded uncertainty set a-priori [3] (a problem in common with robust MPC), which may be difficult to define for a complex real-life system such as a VRE integrated MG operation, which involves a variety of forecasts.

Stochastic MPC (SMPC) methods based on chance constraints strike a trade off between economic operation and full constraint satisfaction [3]. Chance constraints allow for the MPC to operate in a more economical way by respecting a maximum probability of constraint violation. The superior economic performance, lower complexity, and weaker assumption requirements of chance constrained SMPC is desirable for BESS operation in VRE intensive microgrids (MG), especially under uncertainty in VRE and load forecasts, and is thus the primary focus of this work.

B. Literature Review

Chance constrained SMPC algorithms have found applications in problems involving building climate control [3]–[6], optimal power flow [7], and optimal microgrid (MG) dispatch [8]–[18]. Chance-constrained SMPC problems are solved by converting them into an approximate deterministic form. If the uncertainties are Gaussian, or follow other known distributions [19], [20], standard procedures exist to convert the stochastic problem into a deterministic one. However, in real-life scenarios such as VRE and load forecasts, the uncertainty distributions, and additionally, uncertainty statistics (moments like mean, variance, skewness, etc.) may be unknown. Other methods of reformulating the SMPC problem into a deterministic one, such as using Chebyshev inequalities [21] require a-priori knowledge about the uncertainty statistics (mean and covariance), while using Chernoff bounds suffer

from high conservatism [3]. Sampling based approaches [22], [23] suffer from high computational demand and may require a prohibitive number of samples [3]. Chance constraints are generally enforced pointwise-in-time within an MPC prediction horizon, without including past behavior of the system, which can also lead to over-conservativeness (i.e., less than desired constraint violations) in closed-loop. However, reducing over-conservativeness is of paramount importance for MG operators to reduce electricity costs.

The authors in [4] proposed an SMPC approach which enables closed-loop satisfaction of chance constraints. Over-conservativeness, symptomatic in general chance constrained SMPC was avoided by adaptively tightening state constraints during MPC computations based on the past memory of observed constraint violations. The authors, using stochastic approximation, also proved convergence of the time-average of constraint violations in probability to the allowable ‘least conservative’ level. A few limitations of the work is the a-priori assumption of the uncertainty distribution, and the strong assumption of terminal stability region of the state in closed-loop, which is unrealistic for economic MG dispatch using BESS.

The authors in [5] proposed an iterative learning SMPC method based on adaptive constraint tightening to handle chance constraints pointwise-in-time in closed-loop without assuming any a-priori knowledge of the uncertainty distribution or its statistics. The iterative procedure was shown to be equivalent to a root-finding problem and stochastic approximation was applied to show the convergence of the empirical average loss to the prescribed ‘least-conservative’ level in probability. However, a limitation of the method is the assumption that the uncertain sources are highly periodic, which may not hold for VRE and loads in a MG, and may lead to poor economic performance for our application.

The work in [6] also significantly reduced conservatism in chance constrained SMPC in closed-loop by quantifying the amount of violations as a loss function empirically averaged over time. The empirical average loss was weighted by exponential forgetting of past constraint violations. The authors defined a family of stochastic robust control invariant (SRCI) sets for implementing their control online and proved that the empirical weighted average loss is bounded either in expected value or robustly with probability 1, and derived bounds on the convergence time. Drawbacks of the work include high computational cost to parameterize the SRCI sets, and a-priori knowledge about the distribution/statistics of the uncertainty.

Work similar to [6] was done by authors in [24] where chance constrained SMPC was reformulated for online implementation, using the memory of past violations. The authors in [24] proposed two methods imposing a bound on the time-average of (i) number of constraint violations in the first method, and (ii) a loss metric based on a convex loss function of constraint violations in the other method. Instead of providing asymptotic bounds on constraint violations as done in previous works like [3], [4], the authors provided stronger robust bounds in closed-loop over finite time periods. A practical limitation of [24] for our application (economic MG dispatch) is the assumption of an objective function that is composed of

stage costs with quadratic penalties on control inputs and state deviations from an a-priori defined robust positively invariant target set. Construction of a non-conservative robust positively invariant target state set is difficult. Additionally, electricity costs due to grid imports in a MG with BESS cannot be expressed by stage costs with quadratic penalties on control inputs and state deviations, because economic stage costs are not necessarily positive definite with respect to the target set of states and/or control inputs [25].¹

The authors in [27] presented a general non-linear SMPC solution framework involving chance constraints on states. The authors used “polynomial chaos expansions” to propagate the uncertainties through the system model. A limitation of the work is the a-priori assumption of probability distribution function of the uncertainty. The work in [28] presented an SMPC to handle both additive and multiplicative uncertainties. The chance constraints were handled by decomposing the uncertain part of the predicted state into two halves: one, computed offline through a known distribution of the uncertainty, and the other computed online by employing robust tubes. The method ensures satisfaction of the chance constraints in closed-loop. Similar to [24] however, the method in [28] assumes an objective function composed of stage costs quadratic in control inputs and states.

The authors in [3] proposed an online chance constrained SMPC that adaptively tightens the state constraints based on the time-average of past violations. The authors developed an adaptive constraint tightening rule that allows the time-average of violations of the system to converge to the maximum allowable violation probability (interpreted as time-average of violations) in closed-loop. However, as clarified by the authors, the convergence was argued intuitively without rigorous proof. The authors showed the convergence holds for a special simplified class of linear systems subject to the time-average of violations at every time step avoiding a critical region in the neighborhood of the maximum allowable time-average of violations. Thus, the smaller the width of the critical region, the greater are the chances of the system satisfying the conditions necessary for convergence. The advantages of the work lies in its applicability to systems where the uncertainty probability distribution/statistics or periodicity is not assumed. The work also does not need the assumption of terminal stability of the state and the type of the objective function (except convexity assumptions), and the implementation of the SMPC is computationally inexpensive and has similar complexity as that of a nominal MPC. The above mentioned properties make the work in [3] ideal for economic MG dispatch, and forms the primary reference on which we develop our work.

¹Economic MG dispatch involves usage of the electricity cost function directly as the objective function of the MPC controller. Electricity costs incurred by the MG to the utility involve time-of-use energy charges and demand charges. Energy charges (\$/kWh) are incurred based on the volumetric import of electricity from the grid, while demand charges (\$/kW) are incurred based on the maximum load import from the grid over the month. Two distinct time-of-use demand charges are used: one based on maximum grid imports for the whole month called non-coincident demand charge (NCDC), added on top of maximum grid import between 16:00-21:00 h of all days of the month, called on-peak demand charges (OPDC). For commercial and industrial customers, demand charge costs can reach as high as 30-70% of the monthly electricity costs [26].

While significant advancements have been made to develop SMPC with varying degrees of simplifying assumptions, computational cost, and ability to avoid over-conservativeness in closed-loop chance constraint satisfaction, there exists a gap in the literature of exploiting these non-conservative methods for economic MG dispatch under uncertainty. Some recent works involving economic MG dispatch in VRE intensive grids with chance constraints are reviewed below.

The authors in [8] minimized the operational cost of a VRE integrated MG with flexible EV charging that included chance constraints on EV dispatch power and SOC. Flexible EV charging was used for alleviating real-time load and VRE forecast uncertainties. The work in [9] presented an optimal VRE integrated MG scheduling strategy that minimized operational cost subject to chance constraints on islanding capability from the main grid. Islanding capability means that a MG maintains enough spinning reserve (both up and down) to meet local demand and accommodate local VRE after instantaneously disconnecting from the main grid. The authors in [11] presented a SMPC for demand response (DR) for a home energy management system consisting of a PV array, HVAC, BESS, and uncontrollable loads. The controller minimized the PV curtailment and grid import costs with chance constraints ensuring that both DR and thermal comfort conditions are satisfied with a high probability under uncertainties in PV and outdoor temperature forecasts. The authors in [12] proposed a SMPC to minimize grid import costs for a residential DC MG consisting of a PV array, fuel cells, BESS, and load. The MG power exchange with the main grid was reformulated into chance constraints. The authors in [14] presented a day-ahead scheduling framework for multiple MGs under wind, solar, and load forecast uncertainties. The algorithm minimizes the MG operational and emissions costs with chance constraints being considered for the MG power balance. The authors in [15] proposed an optimal VRE integrated MG scheduling model that minimizes MG operational and emissions cost with chance constraints on reserve power constraints.

The authors in [10] proposed a two stage MG scheduling model that minimized operational cost under load and VRE uncertainties. In the day-ahead stage, the uncertainties are modeled using historical data based on a Wasserstein ambiguity set (a ball which contains all possible uncertainty distributions centred at the reference distribution) and a dispatch schedule is generated by solving a distributionally robust chance constrained (DRCC) optimization. In the real-time stage, the deviation of the dispatch schedule from the day-ahead schedule is minimized in an MPC subject to MG constraints. The authors in [13] proposed an evolutionary algorithm that solves a distributionally robust joint chance constrained problem for networked DC MGs. The algorithm optimizes MG operational cost under uncertain VRE forecasts, which is modeled by ambiguity sets from historical data. The authors in [16] presented a non-parametric chance constrained model for day ahead MG scheduling without any a-priori assumption about uncertainty distribution. The algorithm minimizes MG operational costs with chance constraints on the MG electric and thermal power balance, and virtual solar+BESS generator smoothness. The authors used adaptive

kernel density estimation to estimate the nonparametric uncertainty distribution for VRE from historical data, and adjusted the confidence levels according to estimation uncertainties to ensure constraint satisfaction within predefined confidence levels.

None of the above works [8]–[15] considered demand charges in their electricity cost. The work in [8] required extra steps to generate scenarios of uncertainty at every time-step for the MPC prediction horizon and considered the scenarios to be Gaussian. The works [9], [11], [12], [14], [15] considered the uncertainties to be Gaussian or other commonly known distributions, which significantly limits the practical application of these studies. Additionally, the approach in [10], [13], [16] is data-intensive and its performance is substantially influenced by the quality of historical data available.

To tackle the aforementioned problems, [17] and the authors of this paper in a previous work [18] presented an online adaptive SMPC model inspired by [3] that minimized VRE integrated MG operating cost, and satisfied chance constraints on states (BESS SOC) without making any assumption about the probability distribution or statistics of the uncertainty. To further reduce conservativeness under unknown probability distribution of the uncertainty, the works [17], [18] employed adaptive constraint relaxation in the nominal MPC, which to the best of the author’s knowledge was unexplored in the literature, rather than the more common adaptive constraint tightening. However, the online adaptive constraint relaxation rules used in [17] and [18] are based on intuition having no convergence guarantees or theoretical analyses, and both the works are application specific. From an economic MG dispatch perspective, only [18] included demand charges while [17] did not. The authors in [17] used sample historical data of uncertainties for initial constraint relaxation which [18] avoided by practical engineering approximation. The present work is an extension of the previous work [18] by the authors, presented in a more generic setting with additional convergence properties and proofs, related theoretical analyses, and additional case studies.

C. Present Work

In this paper, at first, a generic discrete linear time invariant (LTI) SMPC problem is presented. The SMPC minimizes a generic convex cost function over a finite receding horizon, subject to hard input constraints and chance constraints on states. The chance constraints are interpreted as time-average of state constraint violations in closed loop similar to [3], [4], [6], [24]. These constraints are formulated to allow for a maximum probability of violation in time-average sense by adaptively relaxing the state constraint. The present work does not make a-priori assumptions about the distribution of the uncertainty set or its statistics and does not require sampling from historical data. The SMPC problem is first approximated by framing a nominal (i.e., without uncertainty) convex MPC which adaptively relaxes the state constraints based on the time-average of past violations, and then post-processes the solutions in real-time to account for forecast uncertainties. Second, under an ideal control policy assumption similar

to [3], it is proven that the time-average of constraint violations converges to the maximum allowable probability of constraint violations. The aforementioned convergence of the time-average of the constraint violations allows the SMPC to be non-conservative while also satisfying the chance constraints in closed-loop. Third, the time-average of the constraint violations is proven to asymptotically converge (not necessarily to the maximum allowable violation probability) even without the simplifying assumption, which may be useful for real-life operation of the proposed SMPC to avoid unpredictable violation behavior as the system evolves. Fourth, a case study is presented for a grid connected MG with PV, load, and BESS using realistic data for a full year of operation. In the case study, the optimization problem involves minimizing the electricity cost from grid import online (i.e., in real-time), subject to MG operational constraints (power balance, BESS charging/discharging power limits) with chance constraints being applied on the BESS SOC. The control inputs are the BESS dispatch (i.e., charging/discharging) and grid import power. The case study demonstrates the superior electricity cost saving potential of our proposed method as compared to the traditional MPC (with hard constraints on both inputs and states), while still staying within the maximum violation probability bound. In the end, suggestions are presented to further modify our online adaptive SMPC (OA-SMPC) for the case study which can lead to even greater electricity cost savings.

D. Contributions

The contributions of the present work are as follows:

- 1) The present work proposes a novel OA-SMPC framework to adaptively relax the state constraints for nominal MPC computation, rather than tightening the constraints like most previous works to further aid in reducing conservativeness. To the best of the author’s knowledge, works based on adaptive relaxation for the nominal MPC computation to satisfy chance constraints in closed-loop is limited in the literature. Under the adaptive relaxation rule of the present work, which is updated online based on past constraint violations, it is proven that the time-average of the constraint violations converges to the maximum allowable violation probability under an ideal control policy assumption similar to [3]. However, a rigorous proof is provided here which was not provided in [3]. The critical region for our work, which is related to the convergence properties (see discussion about critical region in Section I-B), is smaller than [3] and allows for more relaxed conditions for guaranteeing convergence.
- 2) The present work also proves the asymptotic convergence of the time-average of the constraint violations even without any simplifying assumptions.
- 3) The present work does not require either any a-priori assumption about the probability distribution of the uncertainty set or its statistics, or sample uncertainties from historical data.
- 4) Previous works considered aggregate constraint violations, without any additional preference for the time when

violations should occur. However, for the case study presented in this work (i.e., economic MG dispatch with demand charges), it becomes critical, if necessary, to preferentially be able to violate BESS state constraints during a predefined on-peak period from 16:00 to 21:00 h, to reduce grid import power peaks, as OPDC (on-peak demand charges levied on the maximum grid import between 16:00-21:00 h of all days of the month) are charged on top of NCDC (non-coincident demand charges levied on the maximum grid import for the whole month). The present work incorporates operational adjustments in the online adaptive relaxation rule to account for temporal preference in state constraint violation. Additionally, unlike the methods in [3], [17], the present method prevents excessive overcharging/overdischarging of the BESS to correct for large forecast uncertainties in real-time by an additional post-processing step, which otherwise might harm the BESS and leave the MG vulnerable for future demand peaks.

- 5) The majority of the earlier works for chance constrained SMPC based economic MG dispatch presented results over a short time (24 h), or one or two months. However, for MG operators, it is important to have at-least year-long studies to determine how the algorithm performs under realistic seasonal variations in loads, VRE generation, and forecasts, a gap which the present work fills.

The rest of the paper is organized as follows. Section II presents the notations and standard definitions. Section III introduces the original SMPC problem formulation with chance constraints, approximates the original formulation to frame the OA-SMPC formulation, along with presenting the convergence proofs and related theoretical analysis. Section IV presents the case study for a realistic grid connected MG with PV, load, and BESS, with results and discussions in Section V. Section VI concludes the paper summarizing the takeaways of the study.

II. MATHEMATICAL PRELIMINARIES

A. Notations

The set of n -tuple of real numbers is denoted by \mathbb{R}^n . Positive and negative real number sets are denoted by \mathbb{R}_{0+} and \mathbb{R}_{0-} , respectively. The set of natural numbers including 0 is denoted by \mathbb{N} . A set of consecutive natural numbers $\{i, i+1, \dots, j\}$ is denoted by \mathbb{N}_i^j . The n tuple of zeros and ones is denoted by $\mathbb{0}^n$ and $\mathbb{1}^n$, respectively. States, control inputs and uncertainties are denoted by $x \in \mathbb{X} \subseteq \mathbb{R}^n$, $u \in \mathbb{U} \subseteq \mathbb{R}^m$, and $w \in \mathbb{W} \subseteq \mathbb{R}^p$ respectively. The prediction horizon of the MPC is denoted by $N \in \mathbb{N}$. Actual states at time $t \in \mathbb{T} \subseteq \mathbb{N}$ are denoted by $x(t)$, while predicted states, obtained at t by MPC computation $k \in \mathbb{N}_1^N$ time-steps in the future are denoted by $x(t+k|t)$. Similarly, predicted control inputs over the MPC prediction horizon are denoted by $u(t+k|t)$, with $k \in \mathbb{N}_0^{N-1}$. An ordered collection of vectors (such as states) over the MPC prediction horizon obtained at time t is denoted by bold letters, $\mathbf{x}(t+1) := (x(t+1|t), x(t+2|t), \dots, x(t+N|t))$. For matrices A and B of equal dimensions, the operators $\{<, \leq, =, >, \geq\}$ hold component wise. The right inverse of a matrix $A \in \mathbb{R}^{m \times n}$ with rank $m < n$ is denoted by A^\dagger . The i^{th} row, and the

element from the i^{th} row and j^{th} column of a matrix A is denoted by A_i and A_{ij} respectively, while the i^{th} element of a vector x is denoted by x_i . The expected value of a random variable Z is denoted by $\mathbb{E}[Z]$. $|x|$ denotes the 1-norm of a vector x .

B. Definitions

Definition 1 (Filtered probability space [29]). A filtered probability space is defined by $(\Omega, \mathcal{F}, \{\mathcal{F}_t\}, \mathbb{P})$. $(\Omega, \mathcal{F}, \mathbb{P})$ is a probability triple with sample space Ω , σ -algebra (event space) \mathcal{F} , and probability measure \mathbb{P} on (Ω, \mathcal{F}) . \mathcal{F}_t is a filtration, which is an increasing family of sub σ -algebras of \mathcal{F} such that $\mathcal{F}_s \subseteq \mathcal{F}_t \subseteq \mathcal{F}$, $\forall t \geq s$, where $t, s \in \mathbb{T}$.

Definition 2 (Almost surely [29]). An event $E \in \mathcal{F}$ happens almost surely if $\mathbb{P}(E) = 1$. It is denoted by a.s.

Definition 3 (Adapted stochastic process [29]). A stochastic process $Z := (Z(t) : t > 0)$, is called adapted to the filtration $\{\mathcal{F}_t\}$ if $Z(t)$ is \mathcal{F}_t measurable $\forall t$.

Definition 4 (Supermartingale [29]). A stochastic process Z is called a discrete-time supermartingale relative to $(\{\mathcal{F}_t\}, \mathbb{P})$ if it satisfies the following:

- (a) Z is an adapted process,
- (b) $\mathbb{E}[|Z(t)|] < \infty$, $\forall t$,
- (c) $\mathbb{E}[Z(t+1)|\mathcal{F}_t] \leq Z(t)$, a.s. $\forall t$.

Definition 5 (Monotone convergence theorem [30]). Let $X = (x_n : n \in \mathbb{N})$ be a sequence of real numbers which is monotonically decreasing in the sense that $x_{n+1} \leq x_n, \forall n$, then the sequence converges if and only if it is bounded, and in which case $\lim_{n \rightarrow \infty} x_n = \inf\{x_n\}$. Similarly, if $X = (x_n : n \in \mathbb{N})$ is a sequence of real numbers which is monotonically increasing in the sense that $x_{n+1} \geq x_n, \forall n$, then the sequence converges if and only if it is bounded, and in which case $\lim_{n \rightarrow \infty} x_n = \sup\{x_n\}$.

III. PROBLEM FORMULATION

A. System Description

The dynamics of the discrete LTI system are governed by

$$x(t+1) = Ax(t) + Bu(t) + Ew(t), \quad \forall t, \quad (1)$$

where $A \in \mathbb{R}^{n \times n}$, $B \in \mathbb{R}^{n \times m}$, and $E \in \mathbb{R}^{n \times p}$.

Assumption 1 (System Dynamics). (a) (A, B) is stabilizable and at each time t , a measurement of the state is available. (b) The set of admissible control inputs \mathbb{U} and states \mathbb{X} are polytopes containing the origin.

Assumption 2 (Uncertainties). The set of uncertainties \mathbb{W} is bounded and contains the origin.

In this setup, $\mathcal{F} = \sigma(\{w : w(t) \in \mathbb{W}\} : t \in \mathbb{T})$, and $\mathcal{F}_t = \sigma(\{w(s) : w(s) \in \mathbb{W}\} : s < t)$. The system is subject to hard control input constraints and chance constraints on states. The control input constraints are formulated as,

$$Su(t) \leq s, \quad \forall t, \quad (2)$$

where $S \in \mathbb{R}^{q \times m}$, $s \in \mathbb{R}^q$. The time-varying equality constraints coupling the control inputs are formulated as,

$$Mu(t) = m(t) + Fw(t), \quad \forall t, \quad (3)$$

where $M \in \mathbb{R}^{d \times m}$, $m \in \mathbb{R}^d$, and $F \in \mathbb{R}^{d \times p}$. In previous works like [3], (3) is not considered but for applications such as economic MG dispatch, (3) is important for incorporating physical constraints such as power balance of the MG with the main grid (discussed in detail in Section III-F). However, if (3) is considered in the problem formulation, the $Ew(t)$ term in the RHS of (1) is dropped as the $Fw(t)$ term in the RHS of (3) accommodates the uncertainty.² Additionally, note that constraint (3) is application specific and is independent of the method and theoretical results presented in this paper. The chance constraints on the states are formulated as,

$$\mathbb{P}[Gx(t) \leq g] \geq \bar{1} - \alpha, \quad \forall t, \quad (4)$$

where $G \in \mathbb{R}^{r \times n}$, $g \in \mathbb{R}^r$ and $\bar{1} \in \mathbb{1}^r$ for individual chance constraints. α is the vector of the pointwise-in-time maximum probability of constraint violation, where $\alpha_i \in (0, 0.5) \forall i \in \mathbb{N}_1^r$. In the individual chance constraint form, (4) can be expressed as, $\mathbb{P}[G_i x \leq g_i] \geq 1 - \alpha_i \forall i \in \mathbb{N}_1^r$. In the joint chance constraint (JCC) form, a single violation probability denoted by $\alpha \in (0, 0.5)$ can be defined for simultaneous satisfaction of all state constraints as,

$$\mathbb{P}[G_1 x \leq g_1, G_2 x \leq g_2, \dots, G_r x \leq g_r]^\top \geq 1 - \alpha.$$

Strictly speaking, the chance constraints are formulated to allow for a maximum probability of violation of state constraints pointwise-in-time. However, for operational purposes, we interpret the probability of violation of state constraints as the time-average of state constraint violations in closed loop similar to [3], [4], [6], [24]. $Gx(t) \leq g$ is referred to as the original constraint with respect to which violations are measured.

B. Online Adaptive SMPC (OA-SMPC)

Over the MPC prediction horizon N , computed from time t , we define the ordered collection of states, control inputs, uncertainties and coupling vectors as,

$$\begin{aligned} \mathbf{x}(t+1) &:= \left(x(t+1|t), x(t+2|t), \dots, x(t+N|t) \right)^\top \in \mathbb{R}^{Nn}, \\ \mathbf{u}(t) &:= \left(u(t|t), u(t+1|t), \dots, u(t+N-1|t) \right)^\top \in \mathbb{R}^{Nm}, \\ \mathbf{w}(t) &:= \left(w(t|t), w(t+1|t), \dots, w(t+N-1|t) \right)^\top \in \mathbb{R}^{Np}, \\ \mathbf{m}(t) &:= \left(m(t|t), m(t+1|t), \dots, m(t+N-1|t) \right)^\top \in \mathbb{R}^{Nd}. \end{aligned}$$

The system dynamics can be written in expanded form as

$$\begin{aligned} x(t+k|t) &= A^k x(t|t) + \sum_{i=0}^{k-1} A^{k-1-i} B u(t+i|t) + \\ &\quad \sum_{i=0}^{k-1} A^{k-1-i} E w(t+i|t), \quad \forall k \in \mathbb{N}_1^N, \forall t, \end{aligned} \quad (5)$$

²The E matrix is still required for assigning a unique control input after accommodating the uncertainty in closed-loop for multi-input systems. See details in Section III-F.

where $x(t|t) = x(t)$. Writing (5) in compact form yields,

$$\mathbf{x}(t+1) = \mathbf{A}\mathbf{x}(t) + \mathbf{B}\mathbf{u}(t) + \mathbf{E}\mathbf{w}(t), \quad \forall t, \quad (6)$$

where $\mathbf{A} \in \mathbb{R}^{Nn \times n}$, $\mathbf{B} \in \mathbb{R}^{Nn \times Nm}$ and $\mathbf{E} \in \mathbb{R}^{Nn \times Np}$.

The hard control input constraints over the MPC prediction horizon are formulated as,

$$S\mathbf{u}(t+k|t) \leq s, \quad \forall k \in \mathbb{N}_0^{N-1}, \forall t. \quad (7)$$

The equality constraints coupling the control inputs over the MPC prediction horizon are formulated as,

$$M\mathbf{u}(t+k|t) = m(t+k|t) + Fw(t+k|t), \quad \forall k \in \mathbb{N}_0^{N-1}, \forall t. \quad (8)$$

Generally, the chance constraints in (4) are interpreted for the MPC prediction horizon pointwise-in-time by (9a), which is over-conservative in closed-loop (see Remark 1). The corresponding relaxed deterministic reformulation of (9a) as implemented in the MPC prediction horizon by some previous works [3], [4] is given by (9b). The aim of the deterministic reformulation is to tighten the state constraints under nominal MPC computations (resulting from ignoring uncertainties, i.e., $\mathbf{w}(t) = \mathbf{0}$) by an adaptive tightening parameter $\tilde{h} \in \mathbb{R}^r$ given by,

$$\mathbb{P}[Gx(t+k|t) \leq g] \geq 1 - \alpha_i, \quad \forall k \in \mathbb{N}_1^N, \forall t, \quad (9a)$$

$$Gx(t+k|t) \leq g - \tilde{h}(t+k|t), \quad \forall k \in \mathbb{N}_1^N, \forall t, \mathbf{w}(t) = \mathbf{0} \quad (9b)$$

where $\tilde{h}_i > 0, \forall i \in \mathbb{N}_1^r$ and is updated based on the time-average of past state constraint violations in closed-loop. Note that violations of state constraints (i.e., $Gx(t) > g$) can occur in closed-loop, as the uncertainties come into effect. The adaptive constraint tightening in (9b) attempts to reduce the conservatism inherent to (9a) by incorporating past state constraint violation behavior of the system in closed-loop, but can still be over-conservative (see Remark 1).

Remark 1 (Over-conservativeness of previous approaches).

(9a) approximates (4) conservatively without considering past state constraint violations [4], [6, Sec. II-A], as (9a) requires the constraint satisfaction conditionally on $x(t)$ (i.e., for $x(t)$ that can be reached at time t by the given control policy under the uncertainty sequence). Equation (4), however, requires constraint satisfaction in a more relaxed average sense (i.e., over all realizations of the uncertainty sequence up to t). Incorporating past constraint violations by using the adaptive tightening in (9b) can still be conservative in satisfying (4) in closed-loop due to the over-estimation of the tightening parameter \tilde{h} [4]. Additionally, in (9b), the nominal MPC solutions never violate the state constraints over the prediction horizon, as a result of restricting the size of the feasible state set (despite a larger feasible state set being available to the controller as compared to the nominal MPC when accommodating for uncertainty), which the MPC optimizer can theoretically exploit to further reduce conservativeness in closed-loop.³

Based on Remark 1, which shows that both (9a) and (9b) can be over-conservative in satisfying (4) in closed-loop, we

³See detailed discussion later in Remark 7.

propose to adaptively relax the state constraints in the nominal MPC instead of tightening them. The adaptive relaxation allows for state constraint violations over the nominal MPC prediction horizon ($Gx(t+k|t) > g$ with $\mathbf{w}(t) = \mathbf{0}$), to *push* the system towards reduced conservativeness. We relax the strict satisfaction of (9a) and approximate (4) by reformulating the nominal state constraints as,

$$Gx(t+k|t) \leq g - h(t), \quad \forall k \in \mathbb{N}_1^N, \forall t, \mathbf{w}(t) = \mathbf{0} \quad (10)$$

where $h \in \mathbb{R}^r$ is the adaptive relaxing parameter with $h_i < 0$, $\forall i \in \mathbb{N}_1^r$. It should be noted that the sign of h_i in (10) is opposite to \tilde{h}_i in (9b). We also observe that decreasing $h(t)$ in (10) expands the feasible state set, pushing the system more towards state constraint violations (i.e., $Gx(t+k|t) > g$), while increasing $h(t)$ contracts the feasible state set pulling the system away from state constraint violations.⁴ The initial value of h at $t = 0$ can be calculated based on domain knowledge [18], which obviates the requirement of past uncertainty samples, as in [3]. The initial value of h is not important since h gets adapted as the system evolves with time [7]. The ordered collection of adaptive relaxation parameters along the MPC prediction horizon is denoted as,

$$\mathbf{h}(t) := \left(h(t), h(t), \dots, h(t) \right)^\top \in \mathbb{R}^{Nr}.$$

The nominal OA-SMPC, which is assumed to be a convex optimization problem is then formulated as,

$$\mathbf{u}^*(t) = \arg \min_{\mathbf{u}(t) \in \mathbb{R}^{Nm}} J(x(t), \mathbf{u}(t), \mathbf{w}(t) = \mathbf{0}) \quad (11a)$$

$$\text{subject to} \quad \mathbf{x}(t+1) = \mathbf{A}\mathbf{x}(t) + \mathbf{B}\mathbf{u}(t) \quad (11b)$$

$$\mathbf{S}\mathbf{u}(t) \leq \mathbf{s} \quad (11c)$$

$$\mathbf{M}\mathbf{u}(t) = \mathbf{m}(t) \quad (11d)$$

$$\mathbf{G}\mathbf{x}(t+1) \leq \mathbf{g} - \mathbf{h}(t) \quad (11e)$$

where $J : \mathbb{R}^n \times \mathbb{R}^{Nm} \times \mathbb{R}^{Np} \rightarrow \mathbb{R}$ is an arbitrary convex function, $\mathbf{S} \in \mathbb{R}^{Nq \times Nm}$, $\mathbf{s} \in \mathbb{R}^{Nq}$, $\mathbf{M} \in \mathbb{R}^{Nd \times Nm}$, $\mathbf{m} \in \mathbb{R}^{Nd}$, $\mathbf{G} \in \mathbb{R}^{Nr \times Nn}$, $\mathbf{g} \in \mathbb{R}^{Nr}$. Note that dropping (11d) makes the problem setup similar to [3].

Assumption 3 (Control inputs [3]). (a) *The control input constraints (11c) are such that the system can overcome the uncertainty from the previous time-step and additionally provide enough control input to bring the state to the feasible region of the OA-SMPC at the next time-step.* (b) *The system is one step controllable.*

Remark 2 (Structure of the input matrix). *Note that Assumption 3(b) is sufficient for saying that the system has at least as many control inputs as states (i.e., $n \leq m$) and B*

⁴Note that in economic MG dispatch with BESS in VRE grids, where the objective function is the actual economic cost of system operation like the electricity bill, and not necessarily only a penalty on the control input (BESS dispatch), relaxing the state constraints in the nominal MPC does not automatically lead the system to predicted nominal solutions that violate the (original) state constraints pathologically over the nominal MPC prediction horizon. The state (BESS SOC), in these applications tries to exploit the full feasible state set to best reduce economic cost for the MPC prediction horizon. Nevertheless, the case where the proposed formulation can result in pathological constraint violations is averted in closed-loop by a post-processing step described later in Section III-F and Remark 9.

has full row rank. The assumption implies that if $n = m$, B has an inverse, while if $n < m$, B has a right inverse.

Note that in (11e), the MPC state constraints are applied for $x(t+k|t) \forall k \in \mathbb{N}_1^N$, and not for the initial state corresponding to $k = 0$. Equation (11e) along with Assumption 3(a) allows for the initial state to be outside of the feasible state set of the MPC, to allow for recursive feasibility of the OA-SMPC [3], allowing for the states to handle uncertainties in closed-loop, and the MPC state constraint limits to contract from one time-step to the other depending on the \mathbf{h} update.

Assumption 4 (Form of the h update rule). *The online h (adaptive relaxing parameter) update rule can be written as $h_i(t) := h_i(t-1)[1 + K_i(t)]$, where $K_i(t) > -1$, $\forall t$ ensures $h_i(t) < 0$, $\forall t$ [18, Eq. (12)].*

Remark 3 (Behavior of the h update rule). *In Assumption 4, $K_i(t) > 0$ decreases $h_i(t)$, expanding the state constraints, pushing the system more towards state constraint violations, while $K_i(t) < 0$ increases $h_i(t)$, contracting the state constraints, pulling the system away from state constraint violations.*

C. Observed Violations

In this section, for consistency with earlier works like [3], we drop (3) and (11d). Thus, the nominal OA-SMPC computed optimal control inputs for the first time-step of the prediction horizon are implemented in closed-loop. The observed states get corrected once the uncertainties are realized, by using (1). The case where (3) and (11d) are considered in the problem formulation is discussed in Section III-F which additionally post-processes the nominal OA-SMPC computed control inputs to correct for the uncertainty.

Without loss of generality, consider the i^{th} state constraint in (4). Let $V_i(t+1) \in \{0, 1\}$ track whether the state constraint is violated in closed-loop at time $t+1$, while $Y_i(t+1) \in [0, 1]$ keeps track of the time-average of violations up to time $t+1$. Note that the control input applied at time t (along with the uncertainty realized at t) is manifested with updated system states, which can be observed only at $t+1$, i.e., there is 1 time-step delay in observing violations (or non-violations) from the time when the control inputs and uncertainties are applied.

$$V_i(t+1) := \begin{cases} 1, & G_i(Ax(t) + Bu^*(t|t) + Ew(t)) > g_i, \\ 0, & G_i(Ax(t) + Bu^*(t|t) + Ew(t)) \leq g_i. \end{cases} \quad (12a)$$

$$Y_i(t+1) := \frac{\sum_{j=1}^{t+1} V_i(j)}{t+1}. \quad (12b)$$

The framework for tracking the state constraint violations and time-average of violations in the case of JCC, is the same as that of the individual chance constraints described in (12). The only difference in the case of JCC is that a violation occurs if any one of the constraints (involved in the JCC) violates its specific state constraint bounds in closed-loop.

D. Convergence Properties of $Y(t)$

In this section, like III-C, without loss of generality, we limit our discussion to the i^{th} state constraint in (4) with

$i \in \mathbb{N}_1^r$, with its corresponding adaptive relaxation parameter $h_i \in \mathbb{R}_{0-}$. The conditions established for ensuring the convergence of the time-average of state constraint violations to the maximum allowable violation probability in this paper uses a similar simplifying assumption as in [3]. The simplifying assumption allows the controller to apply ideal control inputs at the current time-step leading to a desired probability of violation of state constraints at the next time-step, under unknown bounded uncertainties.

Denote by $Z_i(t) = |\alpha_i - Y_i(t)|$ the absolute difference between the maximum allowable violation probability and time-average of violations of the i^{th} state constraint observed at time t . We have to ensure that Y_i tends to α_i in closed-loop as the system evolves with time for non-conservative chance constraint satisfaction. The non-conservative strategy ideally leads to lower costs without violating the state constraints beyond the maximum allowable violation probability.

Theorem 1. *Given $\alpha_i > \frac{1}{2(t_0+1)}$, $Z_i^*(t)$, which is the ideal surrogate of the desired supermartingale $Z_i(t)$, is monotonically decreasing a.s. $\forall t \geq t_0$, if and only if, $Y_i(t) \notin \kappa(\alpha_i, t) \forall t \geq t_0$, where $\kappa(\alpha_i, t)$ is a neighborhood of α_i defined as,*

$$\kappa(\alpha_i, t) := \left(\frac{\alpha_i - \frac{1}{2(t+1)}}{1 - \frac{1}{2(t+1)}}, \frac{\alpha_i}{1 - \frac{1}{2(t+1)}} \right).$$

Proof. As $Z_i(t)$ is non-negative, the convergence of Z_i can be guaranteed a.s., if $Z_i(t)$ is a supermartingale [29]. Following Section II-B, the three conditions for Z_i being a supermartingale are investigated below:

- Let $\mathcal{F}_t = \sigma(\{w(0), w(1), \dots, w(t-1)\})$ be a σ -algebra on uncertainties realized up to time $t-1$. $Z_i(t)$ depends on $Y_i(t)$, which depends on the realization of all the uncertainties up to time $t-1$. Since $Z_i(t)$ is exactly known with information available up to time $t-1$, $Z_i(t)$ is \mathcal{F}_t measurable $\forall t > 0$, and is thus adapted. Also, since $Z_i(t+1)$ is random with information available in \mathcal{F}_t , the process Z_i is stochastic.
- As $V_i(t) \in \{0, 1\}$, $Y_i(t) \in [0, 1]$, and $\alpha_i \in (0, 0.5)$, thus $Z_i(t) = |\alpha_i - Y_i(t)| \in [0, 1]$. Thus, $\mathbb{E}[|Z(t)|] < 1 < \infty \forall t > 0$.
- It remains to show $\mathbb{E}[Z_i(t+1)|\mathcal{F}_t] \leq Z_i(t)$, a.s., $\forall t > 0$, which we will show to hold under similar simplifying assumptions as in [3]. The assumption involves replacing the stochastic $Z_i(t+1)|\mathcal{F}_t$ by its ideal surrogate $Z_i^*(t+1)|\mathcal{F}_t$ as explained next.

From (12b) $Y_i(t+1)$ can be written as,

$$Y_i(t+1) = \sum_{j=1}^{t+1} \frac{V_i(j)}{t+1} = t \frac{Y_i(t)}{t+1} + \frac{V_i(t+1)}{t+1}. \quad (13)$$

Denoting $\mathbb{E}[Z_i(t+1)|\mathcal{F}_t] - Z_i(t)$ by $\Delta_i(t)$ and substituting (13) in $\Delta_i(t)$ results in,

$$\Delta_i(t) = \mathbb{E} \left[\left| \alpha_i - t \frac{Y_i(t)}{t+1} - \frac{V_i(t+1)}{t+1} \right| | \mathcal{F}_t \right] - |\alpha_i - Y_i(t)|. \quad (14)$$

Let $p_i(t+1) := \mathbb{P}(V_i(t+1) = 1 | \mathcal{F}_t)$, which means that $p_i(t+1)$ is the probability of observing a constraint violation

at time $t+1$. Similarly, $1 - p_i(t+1) = \mathbb{P}(V_i(t+1) = 0 | \mathcal{F}_t)$ is the probability of not observing a violation at time $t+1$. We notice that the only stochastic part within the expectation in the RHS of (14) is $V_i(t+1)$ based on \mathcal{F}_t . Therefore, (14) can be rewritten in terms of $p_i(t+1)$ to replace the expectation as,

$$\Delta_i(t) = p_i(t+1) \left[\left| \alpha_i - t \frac{Y_i(t)}{t+1} - \frac{1}{t+1} \right| \right] + (1-p_i(t+1)) \left[\left| \alpha_i - t \frac{Y_i(t)}{t+1} \right| \right] - |\alpha_i - Y_i(t)|. \quad (15)$$

Simplifying yields,

$$\Delta_i(t) = p_i(t+1) \beta_i(t) + \left[\left| \alpha_i - t \frac{Y_i(t)}{t+1} \right| - |\alpha_i - Y_i(t)| \right], \quad (16)$$

$$\beta_i(t) = \left| \alpha_i - t \frac{Y_i(t)}{t+1} - \frac{1}{t+1} \right| - \left| \alpha_i - t \frac{Y_i(t)}{t+1} \right|. \quad (17)$$

To keep the analysis applicable to any arbitrary probability distribution of $w(t)$, we consider the sign of $\beta_i(t)$ to decide the ideal control policy. It is assumed that an ideal control policy exists so that $p(t+1) = p_i^*(t+1)$ where $p_i^*(t+1) = \{0, 1\}$. Specifically, it is assumed that there exists a control input which causes a constraint violation a.s., that is, $p_i^*(t+1) = 1$. Similarly, $p_i^*(t+1) = 0$ means that the controller can drive the system to prevent a constraint violation a.s. We consider $Z_i^*(t)$, and $\Delta_i^*(t)$ where the asterisk has been added to highlight the significance of the assumption. Furthermore, $Z_i^*(t)$ is the ideal surrogate of $Z_i(t)$. We discuss next the ideal control inputs that make $\Delta_i^*(t) \leq 0$ based on the sign of $\beta_i(t)$ [3] and the first term in the RHS of (16). The second and third term in the RHS of (16) is used to derive the critical region $\kappa(\alpha_i, t)$, where despite applying ideal control inputs, $\Delta_i^*(t) > 0$.

When $\beta_i(t) < 0$, we choose ideal control inputs leading to $p_i^*(t+1) = 1$ so that $\Delta_i^*(t)$ may be ≤ 0 a.s. Similarly, if $\beta_i(t) > 0$, then we choose ideal control inputs leading to $p_i^*(t+1) = 0$ so that $\Delta_i^*(t)$ may be ≤ 0 a.s.

The case when $\beta_i(t) = 0$ implies $p_i^*(t+1)$ not having an effect on $\Delta_i(t)$, as the first term in the RHS of (16) vanishes regardless of the value of $p_i(t+1)$. From (17), it can be shown that $\beta_i(t) = 0 \Leftrightarrow Y_i(t) = \frac{\alpha_i - \frac{1}{2(t+1)}}{1 - \frac{1}{(t+1)}}$, and further solving for $\Delta_i(t) > 0$ in (16), yields $\alpha_i > \frac{1}{2(t+1)}$, which becomes more likely to be satisfied as t increases. However, the case $\beta_i(t) = 0$ can be avoided by a particular choice of α_i . From (17),

$$\beta_i(t) \neq 0 \Leftrightarrow Y_i(t) \neq \frac{\alpha_i - \frac{1}{2(t+1)}}{1 - \frac{1}{(t+1)}}.$$

Since, $Y_i(t) = \frac{\sum_{j=1}^t V_i(j)}{t}$, and $\sum_{j=1}^t V_i(j) \in \mathbb{N}$, therefore,

$$Y_i(t) \neq \frac{\alpha_i - \frac{1}{2(t+1)}}{1 - \frac{1}{(t+1)}} \Leftrightarrow \sum_{j=1}^t V_i(j) \neq (t+1)\alpha_i - \frac{1}{2},$$

which can be ensured by appropriate choice of α_i . Specifically, $(t+1)\alpha_i - \frac{1}{2} \notin \mathbb{N} \forall t$.

1) *h update rule*: $\beta_i(t) < 0$ implies $\alpha_i - Y_i(t) + \frac{2Y_i(t)-1}{2(t+1)} > 0$, and is associated with violation of state constraints at $t+1$ which is achieved by expanding the state constraint limits in (11e). Similarly $\beta_i(t) > 0$ implies $\alpha_i - Y_i(t) + \frac{2Y_i(t)-1}{2(t+1)} < 0$ and is associated with non-violation of state constraints at $t+1$ which is achieved by shrinking the limits in (11e). From Assumption 4, the h_i update rule can be framed with $K_i(t) \propto [\alpha_i - Y_i(t) + \frac{2Y_i(t)-1}{2(t+1)}]$ as

$$h_i(t) = h_i(t-1) \left[1 + \frac{\alpha_i - Y_i(t) + \frac{2Y_i(t)-1}{2(t+1)}}{\gamma_i} \right], \quad (18)$$

where γ_i is a constant of proportionality that adjusts the rate of h_i update. The update rule in (18) provides the fastest convergence to α_i and results in the least conservative chance constraint satisfaction under the existence of ideal control inputs. From (18), when $\alpha_i - Y_i(t) + \frac{2Y_i(t)-1}{2(t+1)} > 0$, $h_i(t)$ decreases, which expands the feasible state set, pushing the system towards $p_i(t+1) = 1$. Similarly, when $\alpha_i - Y_i(t) + \frac{2Y_i(t)-1}{2(t+1)} < 0$, $h_i(t)$ increases, which contracts the feasible state set, pushing the system towards $p_i(t+1) = 0$.

2) *Statement of the proof*: Theorem 1 says that given $\alpha_i > \frac{1}{2(t_0+1)}$, $\mathcal{P} \iff \mathcal{Q}$, where \mathcal{P} is defined as $\Delta_i^*(t) \leq 0$ a.s. $\forall t \geq t_0$, and \mathcal{Q} is defined as $Y_i(t) \notin \kappa(\alpha_i, t) \forall t \geq t_0$, where $\kappa(\alpha_i, t)$ is defined as,

$$\kappa(\alpha_i, t) := \left(\frac{\alpha_i - \frac{1}{2(t+1)}}{1 - \frac{1}{2(t+1)}}, \frac{\alpha_i}{1 - \frac{1}{2(t+1)}} \right).$$

To prove, $\mathcal{P} \iff \mathcal{Q}$, we will first prove the inverse as true, i.e., $\neg\mathcal{P} \implies \neg\mathcal{Q}$, which implies $\mathcal{Q} \implies \mathcal{P}$. Then we will prove the contrapositive as true, i.e., $\neg\mathcal{Q} \implies \neg\mathcal{P}$, which implies $\mathcal{P} \implies \mathcal{Q}$, which will complete the proof.

Starting with $\neg\mathcal{P} \implies \neg\mathcal{Q}$, assume $\neg\mathcal{P}$ is true, i.e., $\Delta_i^*(t) > 0$ a.s. To show, $\neg\mathcal{Q}$ holds, we consider Cases 1, 2 and 3 based on the sign of $\beta_i(t)$ below.

Case 1.

$$\begin{aligned} \beta_i(t) < 0 &\Leftrightarrow p_i^*(t+1) = 1 \\ &\Leftrightarrow \alpha_i - Y_i(t) + \frac{2Y_i(t)-1}{2(t+1)} > 0 \Leftrightarrow Y_i(t) < \frac{\alpha_i - \frac{1}{2(t+1)}}{1 - \frac{1}{2(t+1)}}. \end{aligned} \quad (19a)$$

Solving for $\Delta_i^*(t) > 0$ when $p_i^*(t+1) = 1$ yields

$$Y_i(t) > \frac{\alpha_i - \frac{1}{2(t+1)}}{1 - \frac{1}{2(t+1)}}. \quad (19b)$$

Equation (19) implies the critical region of Case 1 is $\kappa_1(\alpha_i, t) = \left(\frac{\alpha_i - \frac{1}{2(t+1)}}{1 - \frac{1}{2(t+1)}}, \frac{\alpha_i - \frac{1}{2(t+1)}}{1 - \frac{1}{2(t+1)}} \right)$, implying if $Y_i(t) \in \kappa_1(\alpha_i, t)$, despite applying ideal control inputs to the system at t leading to $p_i^*(t+1) = 1$, $\Delta_i^*(t) > 0$ a.s.

Case 2.

$$\begin{aligned} \beta_i(t) > 0 &\Leftrightarrow p_i^*(t+1) = 0 \\ &\Leftrightarrow \alpha_i - Y_i(t) + \frac{2Y_i(t)-1}{2(t+1)} < 0 \Leftrightarrow Y_i(t) > \frac{\alpha_i - \frac{1}{2(t+1)}}{1 - \frac{1}{2(t+1)}}. \end{aligned} \quad (20a)$$

Solving for $\Delta_i^*(t) > 0$ when $p_i^*(t+1) = 0$ yields

$$Y_i(t) < \frac{\alpha_i}{1 - \frac{1}{2(t+1)}}. \quad (20b)$$

Equation (20) implies the critical region of Case 2 is $\kappa_2(\alpha_i, t) = \left(\frac{\alpha_i - \frac{1}{2(t+1)}}{1 - \frac{1}{2(t+1)}}, \frac{\alpha_i}{1 - \frac{1}{2(t+1)}} \right)$, implying if $Y_i(t) \in \kappa_2(\alpha_i, t)$, despite applying ideal control inputs to the system at t leading to $p_i^*(t+1) = 0$, $\Delta_i^*(t) > 0$ a.s.

Case 3. $\beta_i(t) = 0$ leads to $\Delta_i^*(t) > 0$ a.s. because $\alpha_i > \frac{1}{2(t_0+1)} \geq \frac{1}{2(t+1)}$, $\forall t \geq t_0$. Additionally, $\beta_i(t) = 0 \Leftrightarrow Y_i(t) = \frac{\alpha_i - \frac{1}{2(t+1)}}{1 - \frac{1}{2(t+1)}} = \kappa_3(\alpha_i, t)$.

The total critical region from Cases 1, 2 and 3 yields,

$$\begin{aligned} \kappa(\alpha_i, t) &= \kappa_1(\alpha_i, t) \cup \kappa_2(\alpha_i, t) \cup \kappa_3(\alpha_i, t) \\ &= \left(\frac{\alpha_i - \frac{1}{2(t+1)}}{1 - \frac{1}{2(t+1)}}, \frac{\alpha_i}{1 - \frac{1}{2(t+1)}} \right), \end{aligned}$$

which shows that if $\Delta_i^*(t) > 0$ a.s., then $Y_i(t) \in \kappa(\alpha_i, t)$, which proves $\neg\mathcal{P} \implies \neg\mathcal{Q}$.

To prove $\neg\mathcal{Q} \implies \neg\mathcal{P}$, assume, $\neg\mathcal{Q}$, i.e. $Y_i(t) \in \kappa(\alpha_i, t)$. $\neg\mathcal{Q}$ is subdivided into Cases 4, 5 and 6.

Case 4. $\beta_i(t) < 0 \Leftrightarrow p_i^*(t+1) = 1$, which yields (19a). (19a) and $Y_i(t) \in \kappa(\alpha_i, t)$ yields, $Y_i(t) \in \left(\frac{\alpha_i - \frac{1}{2(t+1)}}{1 - \frac{1}{2(t+1)}}, \frac{\alpha_i - \frac{1}{2(t+1)}}{1 - \frac{1}{2(t+1)}} \right) = \kappa_1(\alpha_i, t)$. However, from Case 1, we know that when $p_i^*(t+1) = 1$ and $Y_i(t) \in \kappa_1(\alpha_i, t)$, then $\Delta_i^*(t) > 0$ a.s.

Case 5. $\beta_i(t) > 0 \Leftrightarrow p_i^*(t+1) = 0$, which yields (20a). (20a) and $Y_i(t) \in \kappa(\alpha_i, t)$ yields, $Y_i(t) \in \left(\frac{\alpha_i - \frac{1}{2(t+1)}}{1 - \frac{1}{2(t+1)}}, \frac{\alpha_i}{1 - \frac{1}{2(t+1)}} \right) = \kappa_2(\alpha_i, t)$. However, from Case 2, we know that when $p_i^*(t+1) = 0$ and $Y_i(t) \in \kappa_2(\alpha_i, t)$, then $\Delta_i^*(t) > 0$ a.s.

Case 6. $\beta_i(t) = 0 \Leftrightarrow Y_i(t) = \kappa_3(\alpha_i, t)$ which leads to $\Delta_i^*(t) > 0$ a.s. because $\alpha_i > \frac{1}{2(t+1)}$.

Cases 4, 5 and 6 together prove $\neg\mathcal{Q} \implies \neg\mathcal{P}$, which completes the proof. \square

Remark 4 (Implication of Theorem 1). *Theorem 1 establishes the conditions necessary and sufficient for $\Delta_i^*(t) \leq 0$ a.s. $\forall t \geq t_0$, which implies that $Z_i^*(t)$ is monotonically decreasing a.s. $\forall t \geq t_0$. As $Z_i^*(t)$ is bounded from below by 0, i.e. $\inf\{Z_i^*(t)\} = 0$, we conclude $\lim_{t \rightarrow \infty} Z_i^*(t) = 0$ a.s. from the monotone convergence theorem, which implies the convergence of Y_i to α_i a.s., if $\alpha_i > \frac{1}{2(t_0+1)}$, $p_i(t+1) = p_i^*(t+1)$, and $Y_i(t) \notin \kappa(\alpha_i, t) \forall t \geq t_0$.*

Remark 5 (Width of the critical region [3]). *The width of the critical region $\kappa(\alpha_i, t)$ is $\frac{1}{2t+1}$, while $Y_i(t) \in \{0, \frac{1}{t}, \frac{2}{t}, \dots, 1\}$. The granularity in possible values of $Y_i(t)$ is $1/t$, $\forall t$. As $\frac{1}{2t+1} < \frac{1}{t}$, there is at most one critical value of $Y_i(t)$, such that despite adapting the system to take ideal control inputs leading to $p_i(t+1) = p_i^*(t+1)$, it is possible that $\Delta_i^*(t) > 0$ which leads to the deviation of Y_i from α_i momentarily. However, the width of the critical region monotonically decreases as t increases, therefore, the assumption of $Y_i(t) \notin \kappa(\alpha_i, t)$, is weak and can be easily satisfied as t increases. The width*

of the critical region in the present work is also smaller than [3], implying more relaxed conditions for guaranteeing convergence of Y_i to α_i .

Remark 6 (Significance of the h update rule). In general, the ability of the system to adapt at time t to take ideal control inputs such that $p_i(t+1) = p_i^*(t+1)$ based on the information available up to time $t-1$ is a strong assumption and is unrealistic. In real-life, $p_i(t+1) \in [0, 1]$ while ideally $p_i^*(t+1) \in \{0, 1\}$. Thus, Y_i would not necessarily converge to α_i in real-life applications and Z_i is, in general, not a supermartingale. However, the significance of the proposed h (adaptive relaxing parameter) update rule under the simplifying assumption shows that even with adaptive constraint relaxing, as opposed to tightening in [3], we can achieve similar convergence results of Y_i to α_i , under the same strong assumption. Our h update rule, though, differs from [3].

Remark 7 (Non-conservativeness of the proposed method). During correction of the observed states for uncertainties in closed-loop, the previous works [3]–[5] made available a larger feasible state set than what was available in their nominal MPC to satisfy the physical constraints of the system. Specifically, in closed-loop, the state constraints are allowed to be violated beyond the limits set by $\tilde{h}(t)$ in (9b). For example, in an air-conditioning system, the temperature (state) can increase or decrease beyond the limits set by $\tilde{h}(t)$ after weather related uncertainties are realized to satisfy the heat balance [3]–[5]. As the nominal MPC optimizes over a more restricted feasible state set, due to adaptive constraint tightening, than what was available in closed-loop, it can be over-conservative for real-life applications. On the other hand, in our work, the h update rule in (18) is based on constraint relaxation and allows the nominal OA-SMPC to optimize over a larger feasible state set than the nominal MPC in previous works [3]–[5]. Furthermore, the same feasible state set is available to both the nominal OA-MPC and when correcting for disturbances in closed-loop, allowing for lower conservativeness. We introduce a post-processing step in Section III-F that allows the OA-MPC to satisfy the physical constraints of the system in the presence of uncertainties in closed-loop without expanding the feasible state set defined by $h(t)$ in (10).

Lemma 1. Given any initial time t_0 , with $\alpha_i > \frac{1}{2(t_0+1)}$ and $Y_i(t_0) \notin \kappa(\alpha_i, t_0)$, if ideal control inputs are applied at time t such that $p_i(t+1) = p_i^*(t+1) \forall t \geq t_0$, then there exists some time $t' = \inf\{t > t_0 \mid Y_i(t) \in \kappa(\alpha_i, t)\}$ a.s.

Proof. The lemma states that if the initial time-average of violations of state constraints is outside of the critical region, and we apply ideal control inputs from thereon, then at some future time t' , the time-average of violations comes inside the critical region a.s. Lemma 1 implies the a.s. monotonic decrease of $Z_i^*(t)$ is violated for $t > t'$ (see Theorem 1). Lemma 1 can be proved by showing that when $Z_i^*(t)$ decreases, then $\frac{\delta \hat{w}_i(t)}{\delta t} > \frac{\delta Z_i^*(t)}{\delta t}$, where $\hat{w}(t)$ is the width of the critical region at time t , and δ is a finite positive change.

$\hat{w}_i(t) := \frac{1}{2t+1}$, implying $\delta \hat{w}_i(t) := \hat{w}_i(t+1) - \hat{w}_i(t) = \frac{-2}{(2t+1)(2t+3)}$ where $\delta t := 1$. Thus, $\hat{w}_i(t)$ decreases in the order of $\mathcal{O}(\frac{1}{t^2})$.

Similarly, $\delta Z_i^*(t) := Z_i^*(t+1) - Z_i^*(t) = \Delta_i^*(t)$. $\Delta_i^*(t)$ can be subdivided into Cases 1 and 2.

Case 1. When $p_i^*(t+1) = 1$, $\Delta_i^*(t) = \left[\left| \alpha_i - t \frac{Y_i(t)}{t+1} - \frac{1}{t+1} \right| \right] - |\alpha_i - Y_i(t)|$.

Case 2. When $p_i^*(t+1) = 0$, $\Delta_i^*(t) = \left| \alpha_i - t \frac{Y_i(t)}{t+1} \right| - |\alpha_i - Y_i(t)|$.

Substituting $Y_i(t) = \frac{\sum_{j=1}^t V_i(j)}{t}$, where $\sum_{j=1}^t V_i(j) \leq t$, in both Cases 1 and 2, we see that when $Z_i^*(t)$ decreases a.s. by virtue of $Y_i(t) \notin \kappa(\alpha_i, t)$, then $Z_i^*(t)$ decreases most modestly (i.e., with the least magnitude of decrease), in the order of $\mathcal{O}(\frac{1}{t})$, which proves that, $\frac{\delta \hat{w}_i(t)}{\delta t} > \frac{\delta Z_i^*(t)}{\delta t}$, which completes the proof. \square

Lemma 2. Given any initial time t_0 , with $\alpha_i > \frac{1}{2(t_0+1)}$ and $Y_i(t_0) \in \kappa(\alpha_i, t_0)$, if ideal control inputs are applied at time t such that $p_i(t+1) = p_i^*(t+1) \forall t \geq t_0$, then there exists some time $t' = \inf\{t > t_0 \mid Y_i(t) \notin \kappa(\alpha_i, t)\}$ a.s.

Proof. The lemma states that if the initial time-average of violation of state constraints is inside the critical region, and we apply ideal control inputs from thereon, then at some future time t' , the time-average of violation goes outside of the critical region a.s. Lemma 2 prevents the monotonic increase of $Z_i^*(t)$ for $t > t'$. When $Z_i^*(t)$ increases, satisfaction of $\left| \frac{\delta \hat{w}_i(t)}{\delta t} \right| \leq \left| \frac{\delta Z_i^*(t)}{\delta t} \right|$ is sufficient to prove Lemma 2. The proof follows from showing that $\hat{w}_i(t)$ decreases in the order of $\mathcal{O}(\frac{1}{t^2})$, and when $Z_i^*(t)$ increases a.s. by virtue of $Y_i(t) \in \kappa(\alpha_i, t)$, then from Cases 1 and 2 of Lemma 1, $Z_i^*(t)$ increases most modestly in the order of $\mathcal{O}(\frac{1}{t})$, which completes the proof. \square

Theorem 2. Given any initial time t_0 with $\alpha_i > \frac{1}{2(t_0+1)}$, and time-average of violations $Y_i(t_0)$, if ideal control inputs are applied at time t such that $p_i(t+1) = p_i^*(t+1) \forall t \geq t_0$, then Y_i converges to α_i a.s.

Proof. The theorem states that if ideal control inputs are applied to the system starting from any arbitrary time t_0 with $\alpha_i > \frac{1}{2(t_0+1)}$, then the time-average of violations converges to the maximum probability of violations of state constraints a.s. The proof follows from Theorem 1, Lemmas 1, 2, and Remark 5, and relaxes the assumption of $Y_i(t) \notin \kappa(\alpha_i, t) \forall t$, of Theorem 1/Remark 4. Theorem 2 also rigorously proves the result which was intuitively argued in [3].

From Remark 5, the width of the critical region $\hat{w}_i(t)$ is $\frac{1}{2t+1}$, which monotonically decreases with time. As the critical region $\kappa(\alpha_i, t)$ is a neighborhood of α_i by construction, decrease of $\hat{w}_i(t)$ implies decrease of the width of the neighborhood. $\lim_{t \rightarrow \infty} \hat{w}_i(t) = 0$, which implies $\kappa(\alpha_i, t)$ vanishes at $t \rightarrow \infty$. With $\alpha_i > \frac{1}{2(t_0+1)}$ and $p_i(t+1) = p_i^*(t+1) \forall t \geq t_0$, two cases are possible:

Case 1. When $Y_i(t_0) \notin \kappa(\alpha_i, t)$, Lemma 1 concludes that there exists some $t' = \inf\{t > t_0 \mid Y_i(t) \in \kappa(\alpha_i, t)\}$ a.s, which

implies that Y_i is closer to α_i at time t' as compared to t_0 a.s. (see Theorem 1). Then, from Lemma 2, we can conclude that there exists some $t'' = \inf\{t > t' \mid Y_i(t) \notin \kappa(\alpha_i, t)\}$ a.s., and Y_i is farther away from α_i at time t'' as compared to t' a.s. (see Theorem 1). The process repeats, with Y_i coming in and out of the critical region a.s. as time progresses. However, as the critical region monotonically decreases with time and vanishes at $t \rightarrow \infty$, we conclude Y_i converges to α_i a.s.

Case 2. When $Y_i(t_0) \in \kappa(\alpha_i, t)$, a similar argument can be made as in Case 1 involving Lemma 1 and 2, with Y_i coming in and out of the critical region a.s. until ultimately converging to α_i a.s. at $t \rightarrow \infty$.

Both Cases 1 and 2 complete the proof. \square

E. Asymptotic Behavior of the Real Life System

It is important to determine the asymptotic behavior (i.e., as $t \rightarrow \infty$) of the real-life system in which the simplifying assumption of applying an ideal control policy referred to in Section III-D is dropped.

Theorem 3. *The expected value of $Y_i(t+1)|\mathcal{F}_t$ asymptotically converges to $Y_i(t)$.*

Proof. Applying the limit of $t \rightarrow \infty$ to (16), and rearranging to bypass the indeterminate $\frac{\infty}{\infty}$ form, we get,

$$\lim_{t \rightarrow \infty} \Delta_i(t) = \lim_{t \rightarrow \infty} p_i(t+1) \left[\left| \alpha_i - \frac{Y_i(t)}{1 + \frac{1}{t}} - \frac{1}{t+1} \right| - \left| \alpha_i - \frac{Y_i(t)}{1 + \frac{1}{t}} \right| \right] + \left| \alpha_i - \frac{Y_i(t)}{1 + \frac{1}{t}} \right| - |\alpha_i - Y_i(t)| \quad (21)$$

As $p_i(t+1) \in [0, 1]$, substituting $t \rightarrow \infty$ in (21), yields $\lim_{t \rightarrow \infty} \Delta_i(t) = 0$, which implies either:

Case 1. $\lim_{t \rightarrow \infty} Y_i(t) = \lim_{t \rightarrow \infty} \mathbb{E}[Y_i(t+1)|\mathcal{F}_t]$.

Case 2. $\lim_{t \rightarrow \infty} Y_i(t) = \alpha_i + l$ and $\lim_{t \rightarrow \infty} \mathbb{E}[Y_i(t+1)|\mathcal{F}_t] = \alpha_i - l$, where, $l \in [-\alpha_i, \alpha_i]$.

Taking expectation on both sides of (13) yields,

$$\mathbb{E}[Y_i(t+1)|\mathcal{F}_t] = t \frac{Y_i(t)}{t+1} + \mathbb{E} \left[\frac{V_i(t+1)|\mathcal{F}_t}{t+1} \right]. \quad (22)$$

Taking the limit at $t \rightarrow \infty$ in (22), and substituting the values of $\lim_{t \rightarrow \infty} Y_i(t)$ and $\lim_{t \rightarrow \infty} \mathbb{E}[Y_i(t+1)|\mathcal{F}_t]$ yields,

$$\alpha_i - l = \lim_{t \rightarrow \infty} \frac{\alpha_i + l}{1 + \frac{1}{t}} + \lim_{t \rightarrow \infty} \mathbb{E} \left[\frac{V_i(t+1)|\mathcal{F}_t}{t+1} \right]. \quad (23)$$

As $\mathbb{E}[V_i(t+1)|\mathcal{F}_t] = p_i(t+1) \in [0, 1]$, hence evaluating the limit in (23) yields $l = 0$. Hence Case 2 implies Case 1 (but not the other way around).

Case 1 completes the proof. \square

The asymptotic convergence guarantee of the time-average of constraint violations may be useful for real-life operation of the proposed SMPC to avoid unpredictable violation behavior as the system evolves.

F. Post-processing for Real-time System Operation

In previous works such as [3], after the nominal MPC computed optimal control inputs for the first time-step of the prediction horizon are implemented, the observed states get corrected in closed-loop to account for real-time uncertainties by (1). Accommodation of the entire uncertainty (uncertainty in weather forecast) by the state is reasonable for building climate control applications where the state (room temperature) and control input (heating/cooling effect from the air-conditioner) are not coupled to the same physical equipment [3]. However, in certain applications where the states and control inputs are coupled to the same equipment (like BESS, where state of charge (SOC) is the state, and charging/discharging power is a control input), the first time-step optimal control inputs (computed by the MPC) can also be post-processed in real-time to correct for the realized uncertainty. For example, the BESS can alter its MPC computed optimal control inputs and states to correct for the VRE forecast uncertainty in real-time to maintain power balance of the MG with the main grid.

Assumption 5 (Post-processing to correct for uncertainties in real-time). *For each chance constrained state affected by uncertainties: (a) There are two mutually coupled sources of control with one source having the primary responsibility of handling the uncertainties in closed-loop. During correction of the observed states in closed-loop to account for the uncertainty, the feasible altered control input and state set is the same as defined by \mathbf{s}_1 (11c) and $\mathbf{g}_1 - \mathbf{h}_1(t)$ (11e) respectively, which are the time-varying design limitations. The secondary control source always has enough control input available to handle the remaining part of the uncertainty (through satisfaction of (3)) that cannot be handled by the primary source due to the possibility of violation of the time-varying design limitations by the primary control source in closed-loop, (b) The state transition is not dependent on the secondary control source, (c) The primary and secondary control sources are coupled only to each other, (d) The state transition is not dependent on the control sources associated with other states.*

\mathbf{s}_1 is a hard constraint and does not vary with time, but as $\mathbf{h}_1(t)$ is time-varying, we refer to these design limitations as time-varying, when considered together. After updating the states and control inputs, $h(t+1)$ is updated by (18), and the optimization in (11) is repeated. The schematic diagram of the complete OA-SMPC operational framework with post-processing is shown in Fig. 1, with the algorithm presented in Algorithm 1. Note that the results from Theorems 1, 2 and 3 are independent of the post-processing framework, and still hold with post-processing. Additionally, the restrictive one step controllability in Assumption 3(b) can be relaxed for real-life systems while still maintaining the structure of the input matrix in Remark 2 due to Assumption 5.

Example. To demonstrate post-processing, consider a simple system with $x(t) = [x_1(t)]$ as the state subjected to chance constraints, control inputs $u(t) = [u_1(t) \ u_2(t)]^\top$, where u_1 and u_2 are the primary and secondary control sources

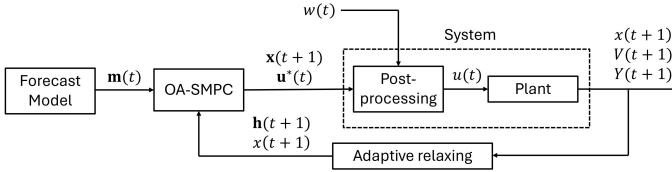


Figure 1. OA-SMPC operational framework with post-processing.

respectively, and the uncertainty is denoted by $w(t)$. The system matrices are A , $B = [B_{11} \ 0]$ and E . The structure of B follows from Assumption 5(b). $u_1(t)$ and $u_2(t)$ are coupled by (3), following Assumption 5(c). Let $\tilde{x}_1(t+1)$ and \tilde{u}_1 be the state and primary control upper limits based on the time-varying design limitations following Assumption 5(a). The system described is similar to a MG with BESS, VRE, local load demand and grid connectivity, where the BESS SOC is the state, BESS charging/discharging power is the primary control source, the grid import forms the secondary control with the control sources coupled by the grid power balance, while the uncertainty is the real-time VRE and load forecast uncertainty.

When correcting for the uncertainties in closed-loop, first it is ensured that the primary control source handles only the part of the uncertainty that still keeps it within the feasible set. The altered primary control input can be formulated as,

$$u_1(t) := \min\left(u_1^*(t|t) + D_1 w(t), \tilde{u}_1\right), \quad (24a)$$

where $D = B^\dagger E$, and $u_1^*(t|t)$ is the optimal MPC computed primary control input. The state update equation using Assumptions 5(a) and 5(b) is formulated as

$$x_1(t+1) = \min\left(Ax_1(t) + B_{11}u_1(t), \tilde{x}_1(t+1)\right). \quad (24b)$$

If from (24b), $x_1(t+1) = \tilde{x}_1(t+1)$, we re-compute, $u_1(t) = (B_{11})^{-1}(\tilde{x}_1(t+1) - Ax_1(t))$. Finally, the altered secondary control input $u_2(t)$ is computed by satisfying (3). In the case of the time-varying design limitations giving the lower limits of the state and primary controls, $\underline{x}_1(t+1)$ and \underline{u}_1 respectively, (24a) and (24b) are modified by replacing the min by the max function. Assumptions 5(a) and 5(b) ensure that the post-processing steps give unique solutions, and Assumptions 5(c) and 5(d) ensure that the correction for uncertainties affecting a chance constrained state and related control inputs does not unnecessarily affect other states and control inputs which may lead to inconsistency in the post-processed solutions. After post-processing, the state constraint violations in closed-loop are tracked as (25) with time-average of violations calculated similar to (12b).

$$V_1(t+1) := \begin{cases} 1, & G_1 x(t+1) > g_1, \\ 0, & G_1 x(t+1) \leq g_1. \end{cases} \quad (25)$$

Remark 8 (Significance of the post-processing framework).

In related previous works with two mutually coupled sources of control to handle uncertainties on chance-constrained states such as [17], the time-varying design limitations as that of Assumption 5(a) are not considered. Large primary control inputs to handle large uncertainties can, thus, potentially lead

to damaging the primary controller in [17]. In other works like [3], MPC computed control inputs are not altered to account for uncertainties, making the state handle the entire uncertainty in closed-loop. Large uncertainties can thus steer the system away from the OA-SMPC feasible region, which due to Assumption 3(a) can lead to the application of expensive control input at the next time-step to bring the system back to feasibility. Such an expensive control input can lead to high economic cost, a problem not considered in both [3] and [17].

Remark 9 (Non-conservative chance constraint satisfaction in ‘practical sense’ in closed-loop even under repeated large uncertainties). *As the nominal OA-SMPC always has access to relaxed feasible states, it is possible for the predicted nominal solutions to always violate the (original) state constraints $\forall k, t$ (as strict satisfaction of (9a) is not mandatory in our formulation). In closed-loop, thus, if solutions are continuously violated more than the maximum prescribed level, h_i increases until $h_i \rightarrow 0^-$ according to (18). Mathematical violations can still persist in $V_i(t+1)$ after $h_i \rightarrow 0^-$ which fails to give the benefit of adaptive relaxation. These violations can be ignored during practical implementation, by adding a small $\varepsilon > 0$ to g_i resulting in considering violations only if $G_i x(t+1) > g_i + \varepsilon$. The consideration of ε in tracking violations is an operational step and can be removed by the user when h_i decreases sufficiently to relax the state constraint and reduce conservatism. This adaptive behavior of our system along with post-processing ensures that the chance constraints in (4) are satisfied in a ‘practical sense’ in closed-loop, which previous works [3], [17] do not consider under repeated large uncertainties, when the mixed worst-case disturbance sequence is not known a-priori. Note that the mixed worst-case disturbance sequence computed via scenarios of uncertainty in [3], [17] may in itself be over-conservative [31].*

Algorithm 1 Online Adaptive SMPC (OA-SMPC)

Initialization

1. Choose $x(0)$.
2. Choose $h(0)$ from domain knowledge.

Online solution

1. Solve (11) to get $u^*(t|t)$.
 - 2a. If post-processing of nominal OA-SMPC computed optimal control inputs are not allowed: Set $u(t) \leftarrow u^*(t|t)$ and account for the uncertainties in $x(t+1)$ by (1). Calculate $V(t+1)$ from (12a).
 - 2b. If post-processing of nominal OA-SMPC computed optimal control inputs are allowed: Post-process by (24) and (3) to account for the uncertainties to calculate $x(t+1)$ and $u(t)$. Calculate $V(t+1)$ similar to (25).
 3. Calculate $Y(t+1)$ from (12b).
 4. Calculate $h(t+1)$ from (18).
 5. Set $t \leftarrow t+1$ and repeat from Step 1 of Online solution.
-

IV. CASE STUDY

A. Overview

In this section, we implement our proposed method (OA-SMPC) for simulating the optimal BESS dispatch strategy for a real-life MG with PV, load and connection to the main grid. The MG setup is from the real-life MG at the Port of San Diego, described in [18]. The MG model incorporates electricity prices with demand and energy charges, realistic load and PV forecast, and a post-processing step for incorporating the forecast uncertainties in BESS dispatch. The yearly (2019) electricity costs were compared for the MG, for the traditional MPC, with hard constraints on the state (BESS SOC), and our OA-SMPC method with chance constraints on the state. The motivation for using chance constraints on BESS SOC in the OA-SMPC is to leverage some extra BESS capacity to reduce demand peaks and thus, demand charges, leading to significant electricity cost savings, while staying within a maximum violation probability bound to avoid adverse effects on BESS life.

B. PV and Load Forecast

The MG model uses day-ahead PV and load forecasts with 15 minute time resolution as inputs. The k-Nearest Neighbor (kNN) algorithm is used for the load forecast. The training data comprises of 15-min resolution historical load observations from November 1, 2018 to November 20, 2019. For every MPC horizon, load observations for the previous 24 h (feature vector) are compared with the training sample and $k=29$ nearest neighbors are identified by the kNN algorithm. Finally, the load forecast is calculated by averaging the load of the selected neighbors at every time-step of the forecast horizon [32].

The PV generation forecast for the upcoming 24 h utilizes the kNN (with $k=30$) algorithm as well. The feature vector is formed by three data sets: numerical weather prediction (NWP) model forecasts for the upcoming 24 h, the average of the preceding 1, 2, 3, and 4 h PV power generation, and the current time of the day. The NWP forecast utilized was the High-Resolution Rapid Refresh (HRRR) model developed by NOAA [33]. The PV power generation dataset was obtained by running simulations for the PV plant in the Solar Advisor Model (SAM) using the irradiance observation data obtained from the NSRDB database as an input. The training sample for PV power generation forecast includes NWP forecast and irradiance observations between January 1, 2019 to December 31, 2019.

C. Microgrid (MG) Model

The system state $x(t) = [x_1(t)]$ is the BESS state of charge (SOC). The control input is $u(t) = [u_1(t) \ u_2(t)]^\top$ where $u_1(t)$ is the BESS dispatch power (primary control source for handling uncertainty), and $u_2(t)$ is the grid import power (secondary control source for handling uncertainty). $u_1(t) > 0$ denotes charging, while $u_2(t) > 0$ denotes power import from the main grid to the MG. The PV generation and gross load is denoted by $PV(t)$ and $L(t)$ respectively and are used as

forecast inputs to the MPC. The uncertainty $w(t) = [w_1(t)]$ is the difference between the PV generation and gross load forecast uncertainties, i.e., $w_1(t) = (PV^r(t) - PV^f(t)) - (L^r(t) - L^f(t))$ where the superscript r and f denote real and forecasted values. The MPC prediction horizon is one-day ahead, subdivided into $N = 96$ equal time-steps of $\Delta t = 0.25$ h (15 minutes) each.

The system matrices are $A = [1]$, $B = [\frac{\Delta t}{\text{BESS}_{\text{en}}} \ 0]$, and $E = [\frac{\Delta t}{\text{BESS}_{\text{en}}}]$ where BESS_{en} is the energy capacity of the BESS. The system matrices handle the SOC update of the battery due to charging/discharging. For the hard control input constraints, $S = \begin{bmatrix} 1 & 0 \\ -1 & 0 \end{bmatrix}$ and $s = [\text{BESS}_{\text{max}} \ \text{BESS}_{\text{max}}]^\top$, which constrains the maximum charging/discharging power of the BESS. For the time varying equality constraints coupling the control inputs, $M = [1 \ -1]$, $m(t) = [PV^f(t) - L^f(t)]$, and $F = [1]$, which ensures power balance of the MG with the main grid. The MPC also has a terminal state constraint defined as $x_1(t+N|t) \geq \hat{x}$.

For this case study, we consider joint chance constraints (JCC) on the BESS SOC which considers a violation if the BESS SOC goes above or below predefined upper (SOC_{max}) and lower bounds (SOC_{min}) in closed-loop. The goal is to reduce electricity import costs from the grid by having controlled violations beyond the predefined upper and lower bounds by making a larger BESS capacity available for dispatch. Unrestricted violations are avoided as they can adversely affect the BESS lifetime. The chance constraints are defined by $G = [1 \ -1]^\top$, $g = [\text{SOC}_{\text{max}} \ -\text{SOC}_{\text{min}}]^\top$ and $h(t) = [h_1(t) \ h_2(t)]^\top$. We choose $h_1(t) = h_2(t)$ for adapting both the state constraints simultaneously by the same parameter as they are setup in JCC form. The maximum probability of the JCC violation is predefined by α . For the traditional MPC (without chance constraints), violations are avoided and the state constraints are formulated as (26), while for the OA-SMPC the state constraints are formulated as (10).

$$Gx(t+k|t) \leq g \quad \forall k \in \mathbb{N}_1^N, \forall t. \quad (26)$$

In the JCC formulation, when updating $h(t)$ by (18), it is ensured that $h_1(t) = \max(\text{SOC}_{\text{max}} - 1, h_1(t))$, and $h_2(t) = \max(-\text{SOC}_{\text{min}}, h_2(t))$ to ensure the state constraints do not violate physical limits of SOC above 1 or below 0. However, in our optimization such violation of physical limits is never encountered, and can be avoided by modest care during design.

The objective function is formulated as in [18], [34], and is given by,

$$J(t) = R_{\text{NC}} \max\{u_2(t+k|t)\}_{k=0}^{N-1} + R_{\text{OP}} \max\{u_2(t+l|t)\}_{l \in \mathbb{I}(t)} + R_{\text{EC}} \Delta t \left[\sum_{k=0}^{N-1} u_2(t+k|t) + \frac{1-\eta}{2} \sum_{k=0}^{N-1} |u_1(t+k|t)| \right], \quad (27)$$

where R_{NC} is the non-coincident demand charge (NCDC) rate charged on the maximum grid import during the prediction horizon. Similarly, R_{OP} is the on-peak demand charge (OPDC) rate, charged on the maximum grid import between 16:00 and 21:00 h, called on-peak (OP) hours of the prediction horizon, and $\mathbb{I}(t)$ represents indices of prediction horizon time-steps coinciding with the OP hours. Naturally, the indices of OP

hours in the prediction horizon are a function of the starting time-step t of the MPC prediction horizon. R_{EC} is the energy charge rate and η is the round-trip efficiency of the BESS accounting for BESS losses. After the net load for the entire month is realized, the monthly NCDC is computed based on maximum load demand from the grid during the month, while the monthly OPDC is computed based on maximum load demand between 16:00 and 21:00 h of all days of the month. The predefined parameters of the MG for the MPC are shown in Table I and a block diagram of the MG operational framework is shown in Fig. 1. Note that the one step controllability in Assumption 3(b) is relaxed for the case study for realistic simulations. The satisfaction of Assumption 3(a) is ensured by modest care in choosing γ which adjusts the rate of $h(t)$ update.

Table I
PARAMETERS FOR THE MG

Parameter	Symbol	Value
NCDC rate	R_{NC}	\$24.48/kW
OPDC rate	R_{OP}	\$19.19/kW
Energy rate	R_{EC}	\$0.1/kWh
BESS round-trip efficiency	η	0.8
BESS energy capacity	$BESS_{en}$	2,500 kWh
BESS power capacity	$BESS_{max}$	700 kW
Upper bound of SOC for traditional MPC	SOC_{max}	0.8
Lower bound of SOC for traditional MPC	SOC_{min}	0.2
Maximum violation probability	α	0.1
Terminal state constraint	\hat{x}	0.5
Initial state	$x_1(0)$	0.5
Initial adaptive parameter	$h(0)$	$[0 \ 0]^T$
Triggering adaptive parameter	$h(t_i)$	$[-0.1 \ -0.1]^T$
Proportionality constant	γ_1 and γ_2	15

D. Operation Strategy

This section presents the real-time operation strategy of the OA-SMPC for the case study under consideration. As the initial state $x(0)$ is far away from the upper/lower limits, we operate the OA-SMPC like a traditional MPC (see $h(0)$ in Table I) until the constraint relaxation is triggered. The constraint relaxation is triggered only when the states reach either the upper or lower limit in closed-loop signifying the possible need for additional BESS capacity. The triggering time is denoted by $t_i = \inf\{t \in \mathbb{N} | x(t) = \{SOC_{min}, SOC_{max}\}\}$, after which the adaptive relaxation parameter is set as $h(t_i)$, which is non-zero, and is subsequently updated in closed-loop by (18). Although (18) updates h at every time-step, given the emphasis on additional OPDC penalties in our cost function, whenever the starting time-step of the MPC coincides with daily OP hours, we restrict the h increase between two time steps, overriding (18) when required. Decreasing h during the daily OP hours is still allowed, and if h increases it is reset manually to the previous value. The reasoning behind restricting the increase of h during OP times is to avoid the additional OPDC costs (on top of NCDC) by incurring preferential violations during OP hours (by deeper BESS

Table II
RESULTS FOR THE 4 TEST CASES FOR THE YEAR 2019. THE COSTS ARE ADDED OVER THE INDIVIDUAL MONTHS TO COMPUTE THE YEARLY COST

Costs	Traditional 1	OA-SMPC 1	Traditional 2	OA-SMPC 2
NCDC	\$66,586	\$65,255	\$57,690	\$64,113
OPDC	\$1,959	\$1,263	\$1,148	\$1,263
Energy Cost	\$14,382	\$14,387	\$14,399	\$14,386
BESS loss	\$8,290	\$8,806	\$10,447	\$9,075
Total Cost	\$91,217	\$89,711	\$83,683	\$88,837
Total BESS cycles	165.8	176.1	208.9	181.5
Y at year end	0%	8.8%	20.4%	10.6%

discharge due to relaxed state constraints). The preferential OP hour violations may lead to state violations beyond the maximum permissible limit temporarily, but the adaptive rule (by virtue of $Y > \alpha$) pushes the BESS to compensate by lowering violations due to rapid increase of h during other times (when risk of penalty on peaks is lower). The simulations are carried out in CVX, a package for solving convex programs in the MATLAB environment [35], [36].

V. RESULTS AND DISCUSSION

We compare results of yearly simulations from 4 test cases: (i) Traditional MPC 1 described in Section IV-C to demonstrate the case without chance constraints; (ii) OA-SMPC 1 described in Section IV-C to demonstrate the case with chance constraints on state; (iii) Traditional MPC 2 which modifies Case (i) with $g = [SOC_{max} - h_1(t_i) \ -SOC_{min} - h_2(t_i)]^T$ to demonstrate the MG performance with the state constraints always relaxed by the same initial triggering parameter in Case (ii) to violate SOC_{max}/SOC_{min} in closed-loop but without adaptation; (iv) OA-SMPC 2 which is a variation of OA-SMPC 1, which is same as OA-SMPC till mid-year (end of June), after which h , t and Y are overridden to their initial values to invoke a restart to the adaptation. The OA-SMPC allows for more aggressive control from the BESS initially when the rate of change of h is significant. However, with the passage of time as Y converges (Theorem 3), the rate of change of h diminishes (see (18)). Case (iv) investigates the effect of invoking a restart to the adaptation on the MG performance when the original rate of change h in Case (ii) is unable to give a reasonable adaptive feedback.

Figure 2 and Table II summarize the simulation results of the 4 test cases for the year 2019. Note that the energy costs are similar across all cases as there is no arbitrage in the MG model. The minute differences in energy costs are due to the different ending BESS SOC at the end of the year for the different test cases.

The comparison between Traditional MPC 1 and OA-SMPC 1 demonstrates the superior economic performance of the chance constrained OA-SMPC algorithm as compared to the Traditional MPC while still staying within the maximum allowable violation probability bound. NCDC and OPDC decrease by 2% and 35.6% between Traditional MPC 1 and OA-SMPC 1. The OPDC savings (as a %) are significantly more than NCDC because of the operation strategy (see Section IV-D) allowing preferential violations during OP hours. As extra BESS capacity is available for the OA-SMPC 1 as compared to the Traditional MPC 1 due to the adaptive relaxation of BESS SOC constraints beyond the 20-80% SOC

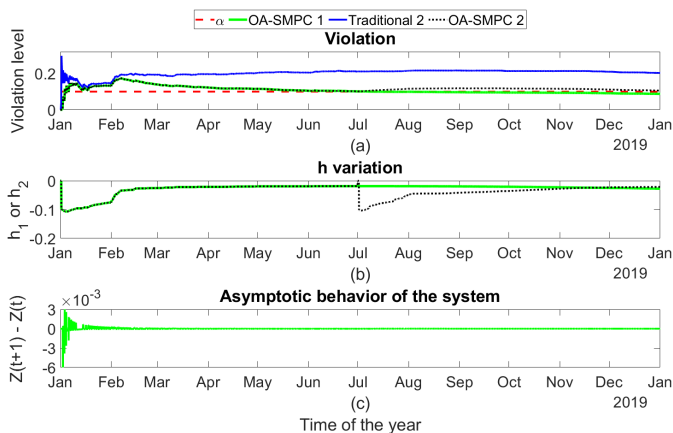


Figure 2. Yearly time-series for the: (a) time-average of state constraint violations (Y) for the OA-SMPC 1, OA-SMPC 2, and Traditional 2 cases studies, and the maximum allowable state constraint violation probability ($\alpha = 10\%$), (b) adaptive state constraint relaxing parameters (h_1 and h_2 , with $h_1 = h_2$ in these case studies) for the OA-SMPC 1 and OA-SMPC 2, (c) adjacent temporal difference of the absolute difference between Y and α for the OA-SMPC 1.

range, the BESS is used more aggressively in OA-SMPC 1 resulting in 6.2% more BESS losses amounting to 10 extra BESS yearly cycles. Overall, OA-SMPC 1 leads to 1.7% total yearly cost savings as compared to the Traditional MPC 1.

Figure 2(a) shows the variation of Y for the OA-SMPC 1 (green line) for the entire year. Initially, Y is 0 until the first constraint violation occurs, after which it overshoots α , oscillating with a high frequency and magnitude until the first week of February. Then, consistent with the goal of Y converging to a probability less than or equal to α , Y decreases, going below α by the middle of the year, and finally reaching a value of 8.8% at the end of the year. The frequency and magnitude of oscillations of over/under shoot of Y with respect to α decreases with time. Figure 2(b) shows that h_1 and h_2 increases and decreases depending on the overshoot and undershoot of Y with respect to α respectively. h_1 and h_2 stabilizes by the middle of March indicating the stability of observed probability of state constraint violations, as proved in Section III-E, and observed graphically in Fig. 2(c).

Traditional MPC 2 demonstrates that relaxing the state (BESS SOC) constraints by the same initial relaxation parameter as in OA-SMPC 1 without any adaptation causes the violations to exceed the maximum allowable violation probability bound in closed-loop (blue line in Fig. 2(a)). The Traditional MPC 2 has lower total yearly electricity costs (due to lower NCDC and OPDC), than OA-SMPC 1 because the objective function in (27) penalizes peaks in grid import power (u_2) more than BESS dispatch power (u_1), resulting in prolonged aggressive dispatch of the BESS to serve the net load ($L - PV$). The aggressive BESS dispatch is more prolonged in Traditional MPC 2 than OA-SMPC 1 because the feasible BESS SOC range in Traditional MPC 2 is not adapted due to past violations, and the feasible state set continues being larger than OA-SMPC 1 throughout. The Traditional MPC 2 shows higher frequency of oscillation and magnitude of overshoot of Y above α as compared to OA-SMPC 1,

and additionally shows that Y consistently remains above 2α for the majority of the year. Thus, the Traditional MPC 2 is unable to fulfill the chance constraints and may significantly harm BESS life, resulting in 33 more yearly BESS cycles as compared to OA-SMPC 1. The analysis serves as a proof of concept that it is the adaptive relaxation rule in OA-SMPC 1 rather than the nature of uncertainties which ensure non-conservative chance constraint satisfaction in closed-loop in OA-SMPC 1.

OA-SMPC 2 (dotted black line in Fig. 2) offers an improvement to the OA-SMPC 1, by invoking a restart to the adaptation when, (i) $Y \rightarrow \alpha$, and (ii) the rate of change of h diminishes to provide reasonable adaptive feedback on constraint relaxation, both of which happens in OA-SMPC 1 by the middle of the year (end of June). The restart to the adaptation allows the OA-SMPC 2 to act more aggressively in violating constraints than OA-SMPC 1, which can be seen in Fig. 2(a) where Y increases once the adaptation is restarted (from the start of July) with h varying more dynamically (see Fig. 2(b)). Table II shows that OA-SMPC 2 reduces NCDC and OPDP costs by 3.7% and 35.6% over Traditional MPC 1, with 9.5% more BESS losses amounting to 15 extra BESS cycles, with a total yearly cost reduction of 2.6%. The cumulative time-average of violations slightly exceeds α at 10.6% at the end of the year. It is expected for Y to come down below α if the OA-SMPC 2 is run over a longer time period, resulting in satisfying the chance constraints, albeit non-conservatively, in closed-loop.

VI. CONCLUSIONS AND FUTURE WORK

This work presents a novel online adaptive state constraint relaxation based stochastic MPC (OA-SMPC) framework for non-conservative chance constraint satisfaction in closed-loop. An adaptive state constraint relaxation rule is developed for a generic discrete LTI system based on the time-average of past constraint violations without any a-priori assumptions about the type and probability distribution of the uncertainty set or its statistics, or sample uncertainties from historical data. The time-average of state constraint violations, under the assumption of ideal control inputs which can cause/prevent constraint violations almost surely, is proven to converge to the maximum allowable violation probability. The time-average of state constraint violations is also proven to asymptotically converge even without the simplifying assumptions.

The proposed method (OA-SMPC) is applied for minimizing monthly electricity costs by optimal BESS dispatch for a grid connected MG at the Port of San Diego using realistic PV and load forecast data for the year 2019. Chance constraints are applied on the BESS SOC to make use of excess BESS capacity in our proposed OA-SMPC as compared to the traditional MPC (which uses hard constraints on BESS SOC), while still remaining within the maximum allowable SOC constraint violation probability bound. The OA-SMPC outperforms the traditional MPC, striking an effective trade off between high BESS utilization and full SOC constraint satisfaction, thereby lowering MG electricity costs by non-conservative chance constraint satisfaction in closed-loop with minimal adverse effect on BESS lifetime.

The analysis involves a trade off between MG electricity cost savings and BESS lifetime, by adaptively relaxing the BESS SOC constraints (which decreases electricity costs by more aggressive BESS discharge, which in turn shortens BESS lifetime). Future work will incorporate the BESS degradation cost and a life-cycle analysis of the MG.

REFERENCES

- [1] P. Kou, F. Gao, and X. Guan, "Stochastic predictive control of battery energy storage for wind farm dispatching: Using probabilistic wind power forecasts," *Renewable Energy*, vol. 80, pp. 286–300, aug 2015.
- [2] S. Singh, M. Pavone, and J.-J. E. Slotine, "Tube-based mpc : a contraction theory approach," 2016.
- [3] F. Oldewurtel, D. Sturzenegger, P. M. Esfahani, G. Andersson, M. Morari, and J. Lygeros, "Adaptively constrained stochastic model predictive control for closed-loop constraint satisfaction," in *American Control Conference*, 2013, pp. 4674–4681.
- [4] D. Muñoz-Carpintero, G. Hu, and C. J. Spanos, "Stochastic model predictive control with adaptive constraint tightening for non-conservative chance constraints satisfaction," *Automatica*, vol. 96, pp. 32–39, 2018.
- [5] Y. Long and L. Xie, "Iterative learning stochastic mpc with adaptive constraint tightening for building hvac systems," *IFAC-PapersOnLine*, vol. 53, no. 2, pp. 11577–11582, 2020.
- [6] M. Korda, R. Gondhalekar, F. Oldewurtel, and C. N. Jones, "Stochastic mpc framework for controlling the average constraint violation," *IEEE Transactions on Automatic Control*, vol. 59, no. 7, pp. 1706–1721, 2014.
- [7] F. Oldewurtel, L. Roald, G. Andersson, and C. Tomlin, "Adaptively constrained stochastic model predictive control applied to security constrained optimal power flow," in *American Control Conference*, 2015, pp. 931–936.
- [8] X. Guo, Z. Bao, H. Lai, and W. Yan, "Model predictive control considering scenario optimisation for microgrid dispatching with wind power and electric vehicle," *The Journal of Engineering*, vol. 2017, no. 13, pp. 2539–2543, 2017.
- [9] G. Liu, M. Starke, B. Xiao, X. Zhang, and K. Tomovic, "Microgrid optimal scheduling with chance-constrained islanding capability," *Electric Power Systems Research*, vol. 145, pp. 197–206, Apr 2017.
- [10] Z. P. Yuan, J. Xia, and P. Li, "Two-Time-Scale Energy Management for Microgrids with Data-Based Day-Ahead Distributionally Robust Chance-Constrained Scheduling," *IEEE Transactions on Smart Grid*, vol. 12, no. 6, pp. 4778–4787, Nov 2021.
- [11] K. Garifi, K. Baker, B. Touri, and D. Christensen, *Stochastic Model Predictive Control for Demand Response in a Home Energy Management System; Stochastic Model Predictive Control for Demand Response in a Home Energy Management System*, 2018.
- [12] M. Gulin, J. Matusko, and M. Vasak, "Stochastic model predictive control for optimal economic operation of a residential dc microgrid," vol. 2015-June. Institute of Electrical and Electronics Engineers Inc., 6 2015, pp. 505–510.
- [13] Y. Ding, T. Morstyn, and M. D. McCulloch, "Distributionally robust joint chance-constrained optimization for networked microgrids considering contingencies and renewable uncertainty," *IEEE Transactions on Smart Grid*, vol. 13, no. 3, pp. 2467–2478, 2022.
- [14] F. H. Aghdam, N. T. Kalantari, and B. Mohammadi-Ivatloo, "A stochastic optimal scheduling of multi-microgrid systems considering emissions: A chance constrained model," *Journal of Cleaner Production*, vol. 275, p. 122965, 2020.
- [15] H. Wang, H. Xing, Y. Luo, and W. Zhang, "Optimal scheduling of micro-energy grid with integrated demand response based on chance-constrained programming," *International Journal of Electrical Power & Energy Systems*, vol. 144, p. 108602, 2023.
- [16] O. Ciftci, M. Mehrtash, and A. Kargarian, "Data-driven nonparametric chance-constrained optimization for microgrid energy management," *IEEE Transactions on Industrial Informatics*, vol. 16, no. 4, pp. 2447–2457, 2019.
- [17] X. Guo, Z. Bao, Z. Li, and W. Yan, "Adaptively Constrained Stochastic Model Predictive Control for the Optimal Dispatch of Microgrid," *Energies 2018, Vol. 11, Page 243*, vol. 11, no. 1, p. 243, Jan 2018.
- [18] A. Ghosh, C. Cortes-Aguirre, Y.-A. Chen, A. Khurram, and J. Kleissl, "Adaptive chance constrained mpc under load and pv forecast uncertainties," in *2023 IEEE PES Grid Edge Technologies Conference & Exposition (Grid Edge)*. IEEE, 2023, pp. 1–5.
- [19] B. Kouvaritakis, M. Cannon, and D. Muñoz-Carpintero, "Efficient prediction strategies for disturbance compensation in stochastic mpc," *International Journal of Systems Science*, vol. 44, no. 7, pp. 1344–1353, 2013.
- [20] B. Kouvaritakis, M. Cannon, S. V. Raković, and Q. Cheng, "Explicit use of probabilistic distributions in linear predictive control," *Automatica*, vol. 46, no. 10, pp. 1719–1724, 2010.
- [21] M. Farina, L. Giulioni, L. Magni, and R. Scattolini, "An approach to output-feedback mpc of stochastic linear discrete-time systems," *Automatica*, vol. 55, pp. 140–149, 2015.
- [22] G. C. Calafiore and L. Fagiano, "Stochastic model predictive control of lqv systems via scenario optimization," *Automatica*, vol. 49, no. 6, pp. 1861–1866, 2013.
- [23] D. Bernardini and A. Bemporad, "Scenario-based model predictive control of stochastic constrained linear systems," in *Proceedings of the 48th IEEE Conference on Decision and Control (CDC) held jointly with 2009 28th Chinese Control Conference*. IEEE, 2009, pp. 6333–6338.
- [24] J. Fleming and M. Cannon, "Time-average constraints in stochastic model predictive control," in *2017 American Control Conference (ACC)*. IEEE, 2017, pp. 5648–5653.
- [25] J. B. Rawlings, D. Angeli, and C. N. Bates, "Fundamentals of economic model predictive control," in *2012 IEEE 51st IEEE conference on decision and control (CDC)*. IEEE, 2012, pp. 3851–3861.
- [26] S. Mullendore, "An introduction to demand charges," *Clean Energy Group, National Renewable Energy Laboratory (NREL)*, 2017.
- [27] A. Mesbah, S. Streif, R. Findelsen, and R. D. Braatz, "Stochastic nonlinear model predictive control with probabilistic constraints," in *2014 American control conference*. IEEE, 2014, pp. 2413–2419.
- [28] Q. Cheng, M. Cannon, B. Kouvaritakis, and M. Evans, "Stochastic mpc for systems with both multiplicative and additive disturbances," *IFAC Proceedings Volumes*, vol. 47, no. 3, pp. 2291–2296, 2014.
- [29] D. Williams, *Probability with martingales*. Cambridge university press, 1991.
- [30] R. G. Bartle and R. G. Bartle, *The elements of real analysis*. Wiley New York, 1964, vol. 2.
- [31] M. Lorenzen, F. Dabbene, R. Tempo, and F. Allgöwer, "Constraint-tightening and stability in stochastic model predictive control," *IEEE Transactions on Automatic Control*, vol. 62, no. 7, pp. 3165–3177, 2016.
- [32] R. Zhang, Y. Xu, Z. Y. Dong, W. Kong, and K. P. Wong, "A composite k-nearest neighbor model for day-ahead load forecasting with limited temperature forecasts," vol. 2016-November. IEEE Computer Society, 11 2016.
- [33] S. G. Benjamin, S. S. Weygandt, J. M. Brown, M. Hu, C. R. Alexander, T. G. Smirnova, J. B. Olson, E. P. James, D. C. Dowell, G. A. Grell, H. Lin, S. E. Peckham, T. L. Smith, W. R. Moninger, J. S. Kenyon, and G. S. Manikin, "A north american hourly assimilation and model forecast cycle: The rapid refresh," *Monthly Weather Review*, vol. 144, no. 4, pp. 1669 – 1694, 2016.
- [34] A. Ghosh, M. Z. Zapata, S. Silwal, A. Khurram, and J. Kleissl, "Effects of number of electric vehicles charging/discharging on total electricity costs in commercial buildings with time-of-use energy and demand charges," *Journal of Renewable and Sustainable Energy*, vol. 14, no. 3, 2022.
- [35] M. Grant and S. Boyd, "CVX: Matlab software for disciplined convex programming, version 2.1," <http://cvxr.com/cvx>, Mar. 2014.
- [36] —, "Graph implementations for nonsmooth convex programs," in *Recent Advances in Learning and Control*, ser. Lecture Notes in Control and Information Sciences, V. Blondel, S. Boyd, and H. Kimura, Eds. Springer-Verlag Limited, 2008, pp. 95–110, http://stanford.edu/~boyd/graph_dcp.html.